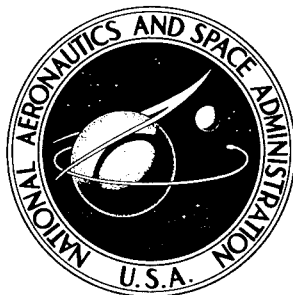


NASA TECHNICAL NOTE



NASA TN D-3919

NASA TN D-3919

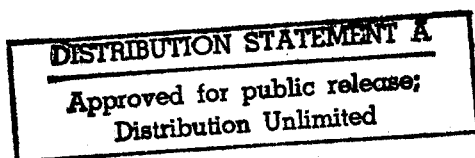
19960402 029

DETERMINATION OF KINETIC PARAMETERS  
OF SIX ABLATION POLYMERS BY  
THERMOGRAVIMETRIC ANALYSIS

by James B. Nelson

Langley Research Center

Langley Station, Hampton, Va.



DTIC QUALITY INSPECTED 1

NATIONAL AERONAUTICS AND SPACE ADMINISTRATION • WASHINGTON, D. C. • APRIL 1967

DEPARTMENT OF DEFENSE  
ELASTICS TECHNICAL EVALUATION CENTER  
PICATINNY ARSENAL, DOVER, N. J.

PIASTEC0317

NASA TN D-3919

DETERMINATION OF KINETIC PARAMETERS OF SIX ABLATION POLYMERS  
BY THERMOGRAVIMETRIC ANALYSIS

By James B. Nelson

Langley Research Center  
Langley Station, Hampton, Va.

NATIONAL AERONAUTICS AND SPACE ADMINISTRATION

For sale by the Clearinghouse for Federal Scientific and Technical Information  
Springfield, Virginia 22151 - CFSTI price \$3.00

# DETERMINATION OF KINETIC PARAMETERS OF SIX ABLATION POLYMERS

## BY THERMOGRAVIMETRIC ANALYSIS

By James B. Nelson  
Langley Research Center

### SUMMARY

Six polymers used in ablation heat-shield composites were investigated by thermogravimetric analysis (TGA) at temperature-rise rates of  $3^{\circ}$  K per minute to  $18^{\circ}$  K per minute in vacuum. These materials were nylon, silicone, polyformaldehyde, and three phenolics. Empirical kinetic parameters were determined for these materials by five different methods (all based on an Arrhenius relation): a direct-solution method, an integral method, a maximum-decomposition method, a multiple-heating-rate method, and a difference method. A best set of parameters was determined for each material by comparing experimental TGA curves with TGA curves derived from the parameters found by each method. The kinetic parameters for the individual materials were shown to satisfactorily describe the mass loss of two composite materials of current interest, a low-density phenolic-nylon and a low-density phenolic-silicone. Direct solution was found to be the most satisfactory method.

### INTRODUCTION

Ablative materials are in common use for the thermal protection of vehicles entering the atmosphere at hypersonic velocities. A type of ablative material which has proven effective over a wide range of environmental conditions is the plastic composite. The mechanisms by which ablative materials provide thermal protection are highly complex and include heat rejection through reradiation, transpiration of gases formed by degradation of the materials, insulation, heat absorption due to the heat capacity of the materials, and the latent heat of thermal degradation.

The behavior of thermal-protection materials is generally determined from investigations in ground-based facilities. Results of these investigations together with a knowledge of certain thermophysical properties of the materials can then be used in theoretical analyses to predict the performance of the materials during atmospheric entry. As shown in references 1 and 2, such analyses require a knowledge of the kinetic parameters describing the mass losses due to thermal degradation.

Many investigators have fitted a single set of kinetic parameters to a composite or to an individual polymer that degrades in two or more obvious steps. Such a degradation cannot be described by a single set of kinetic parameters except in a crude fashion. The purpose of this investigation was to determine the kinetic parameters necessary for a complete description of the mass-loss processes of each material, both alone and in composites.

Information on the degradation mass losses of these polymers was obtained by using the technique of thermogravimetric analysis (TGA). In TGA, sample-weight changes are recorded as functions of temperature while the temperature is increased at a constant rate. By assuming the degradation processes to be approximately governed by a classical pseudo-order kinetic expression, rate parameters are evaluated. These parameters represent the experimental results, but no attempt was made to verify their applicability to conditions other than the experimental test conditions.

### SYMBOLS

The physical quantities defined in this paper are given in the International System of Units (SI). Reference 3 presents factors relating this system to other frequently used systems.

A	frequency factor, per minute
E	activation energy, joules/mole
$-Ei(-X)$	exponential integral, $\int_{\infty}^X X^{-1} e^{-X} dX$
$f\left(\frac{m}{m_0}\right)$	function of mass of undegraded material
K	integral parameter, $-\frac{1}{m_0} \int_{m_0}^m \left(\frac{m - m_r}{m_0}\right)^{-n} dm$
k	specific rate, per minute
i	reaction designation
m	total mass of material at temperature T, milligrams
$m_i$	mass of material in reaction i at temperature T for $i = 1, 2, \dots$ , milligrams

$m_m$	mass of material at maximum rate of mass loss, milligrams
$m_o$	total original mass of material, milligrams
$m_{o,i}$	original mass of material in reaction $i$ for $i = 1, 2, \dots$ , milligrams
$m_r$	mass of residue or char, milligrams
$m_{r,i}$	mass of residue or char for material in reaction $i$ for $i = 1, 2, \dots$ , milligrams
$m_{T=0}$	mass of material at $T = 0$
$n$	pseudo-order of reaction
$p(X) = X^{-1}e^{-X} - (-Ei(-X))$	
$q(X) = X^{-2}e^{-X}$	
$R$	gas constant, 8.3143 joules/mole-°K
$r = \frac{p(X)}{q(X)}$	
$t$	time, minutes
$T$	temperature, °K
$T_m$	temperature at maximum rate of mass loss, °K
$\dot{T}$	temperature-rise rate, $\frac{dT}{dt}$ , °K/minute
$X = \frac{E}{RT}$	
$\left(\frac{dm}{dT}\right)_{\max}$	maximum rate of mass loss

## APPARATUS

A standard laboratory vacuum thermobalance was used to obtain the mass-loss data. A schematic of this instrument is shown in figure 1. The thermobalance continuously records mass changes of a sample being heated from ambient temperature to 1273° K at each of the six selected temperature-rise rates. These rates range from 3° K per minute to 18° K per minute. The pressure of the sample-chamber atmosphere can be controlled from approximately 13 N/m<sup>2</sup> (0.1 torr) to ambient pressure. Sample temperature is measured by a thermocouple located approximately 1 centimeter below the normal position of the sample. This instrument has been described in detail in reference 4.

Associated with the thermobalance is an electronic operational-amplifier differentiator, designed and built at Langley Research Center. This instrument is electrically connected to the thermobalance to give a continuous record of mass-loss rate as a function of time and temperature.

## MATERIALS

The materials in this investigation are commercially available products currently in use at Langley Research Center for the fabrication of composite ablative heat-shield specimens. The individual polymers were processed in the same manner as they would be if incorporated into a composite. The materials are therefore similar to the polymers in the composites but may differ from ideal laboratory polymers in their thermal behavior. A list of the materials tested and of the processing conditions is given in table 1. The nylon and phenolic II are frequently used as fillers in ablative composites formed from phenolics I and III and therefore were subjected to the same postcure conditions as phenolics I and III.

TABLE 1.- EXPERIMENTAL MATERIALS

Material	Description	Resin system	Catalyst	Cure cycle		Postcure cycle	
				Time, hr	Temperature, °K	Time, hr	Temperature, °K
Phenolic I	General-purpose novolac resin	Union Carbide "Bakelite" phenolic resin BRP-5549	Hexamethylenetetramine	1	440	10	365 390 420
Phenolic II	Cured hollow spheres	Microballoons made of Union Carbide BJO-0930 phenolic resin	-----	--	---	10	365 390 420
Phenolic III	Liquid casting resin	Evercoat Chemical EC-251	Amine	1	440	10	365 390 420
Nylon	Nylon 66	DuPont "Zytel" 103 nylon powder	-----	--	---	10	365 390 420
Silicone	Dimethyl polysiloxane	General Electric RTV-602 silicone potting compound	General Electric SRC-04	20	340	4	365
Polyformaldehyde	Polyoxymethylene	DuPont "Delrin"	-----	--	---	--	---

## PREPARATION OF SAMPLES

All specimens used in this study were tested in a powdered form with the exception of phenolic II, which was already in the form of tiny hollow spheres. Powders of phenolics I and III were produced by filing postcured blocks of the materials and collecting the filings. The nylon and polyformaldehyde were ground under liquid nitrogen by the vendor. Pulverizing the silicone polymer proved to be more difficult. This polymer does not become hard enough, even at liquid-nitrogen temperatures, for effective grinding. Small particle sizes of the silicone resin were obtained by casting a mixture (by mass) of about 70 percent silicone resin and about 30 percent hollow silica microspheres. Silica is inert to silicone resins and is widely used as a filler in these resins (ref. 5). The resulting block was largely microspheres coated with a thin film of silicone resin. This block was then filed lightly to yield a fine-particle-size mixture of resin and silica microspheres.

## PROCEDURE

The powdered specimens were dried in a vacuum oven at  $363^{\circ}\text{K}$  before being used. The materials were weighed in an outgassed porcelain crucible by using an analytical balance with a precision of  $\pm 0.1$  milligram. The mass of the specimens was either 100 milligrams or 200 milligrams. The crucible with the sample was placed in the quartz crucible holder of the thermobalance and the furnace tube placed around it. The balance was then calibrated by adding and subtracting weights and adjusting the X-Y recorder to give the desired response. Simultaneously, the mass-loss channel of the differentiator recorder was calibrated. Next a voltage ramp was substituted for the balance signal and the differentiator response noted. The furnace tube was evacuated to approximately  $65\text{ N/m}^2$  (0.5 torr) and the balance rezeroed. The furnace was then raised around the furnace tube and programed to yield a constant temperature-rise rate. Temperature-rise rates ranged from  $3^{\circ}\text{K}$  per minute to  $18^{\circ}\text{K}$  per minute with a rate of  $9^{\circ}\text{K}$  per minute being the most commonly used. After completion of a test, the specimen residue, if any, was weighed by using the analytical balance.

The sample thermocouple in the furnace tube was calibrated periodically by locating one leg of a differential thermocouple in the sample and positioning the other leg with the sample thermocouple. This procedure yielded temperature corrections as functions of indicated temperature for each material at each mass and each temperature-rise rate.

A typical example of the corrections is shown in figure 2. The balance was tared for each test to place the crucible at approximately the same position relative to the sample thermocouple in order to minimize the error in the temperature calibration.

## METHODS OF ANALYSIS

Most polymers degrade in a highly complex manner. These complex degradation mechanisms are generally not understood sufficiently to formulate exact analytical expressions. Therefore, empirical homogeneous kinetics are normally used to describe the degradation.

The thermal degradation mass-loss reactions, if assumed to be irreversible, may be described by the form of the psuedo-order classical rate expression

$$-\frac{1}{m_o} \frac{dm}{dt} = kf\left(\frac{m}{m_o}\right) \quad (1)$$

where the specific rate  $k$  is expressed by the Arrhenius relation

$$k = Ae^{-E/RT} \quad (2)$$

The function  $f(m/m_o)$  usually has the form

$$f\left(\frac{m}{m_o}\right) = \left(\frac{m - m_r}{m_o}\right)^n \quad (3)$$

Equations (1), (2), and (3) may be combined to yield

$$-\frac{1}{m_o} \frac{dm}{dt} = \left(\frac{m - m_r}{m_o}\right)^n Ae^{-E/RT} \quad (4)$$

The kinetic parameters – activation energy  $E$ , frequency factor  $A$ , and order  $n$  – may be determined from this rate equation by using thermogravimetric-analysis data. There are numerous techniques for evaluating these parameters. The five methods used in this paper are representative of the different techniques in current use and are described in detail in appendix A. These methods are as follows: (1) Direct-solution method, (2) Integral method, (3) Maximum-decomposition method, (4) Multiple-heating-rate method, and (5) Difference method.

In order to determine the kinetic parameters  $E$  and  $A$  by the direct-solution, integral, and maximum-decomposition methods, a value for the order  $n$  must be assumed. The difference and multiple-heating-rate methods determine  $n$  as well as  $E$  and  $A$ . Therefore, the value of  $n$  determined by one or both of the latter methods was often used as a basis for assumed values of  $n$  for the other three methods. Kinetic parameters were computed by the direct-solution, integral, and maximum-decomposition



methods for a range of values of  $n$  near the value found by the multiple-heating-rate and difference methods. With the direct-solution and integral methods, the selection of the best set of parameters was aided by noting how linear the Arrhenius plots were for each value of  $n$ . The final check, however, was obtained by computing a TGA plot from the calculated parameters and by comparing this computed plot with an experimental TGA plot. Equations (24), (25), and (27), developed in appendix B, were used to compute the plot.

Many polymers degrade in two or more obvious mass-loss steps. Such degradations cannot be described by a single set of kinetic parameters, except in a crude fashion. Each step must be analyzed as an individual reaction. In order to derive kinetic parameters for these individual steps, it is necessary to know the mass involved in each step. Usually, the mass fractions cannot be determined directly from the TGA mass-loss curve because of overlapping. In the present investigation, this information was obtained from the TGA rate curve in the manner illustrated in figure 3. It can be seen that the mass fractions involved in each reaction can be approximated by extrapolating the individual-reaction-rate curve to zero and graphically integrating.

## RESULTS AND DISCUSSION

The TGA data for the materials tested were analyzed by all the methods described herein. The various parameters found to describe the experimental data most accurately for the six materials are summarized in table 2. Averaged values of the parameters for the individual materials are given in tables 3 to 8, where omissions occur because the determined values varied so widely from one test to another that a meaningful average could not be taken or because, especially with the difference method, the data scatter made it impossible to compute any values at all. Direct solution proved to be the most consistently accurate method.

TABLE 2.- SUMMARY OF KINETIC PARAMETERS GIVING  
BEST FIT WITH EXPERIMENTAL DATA

Material	Reaction no.	E, kJ/mole	A, min <sup>-1</sup>	n	$\frac{m_{O,i}}{m_O}$	$\frac{m_{F,i}}{m_O}$	Method
Phenolic I	1	115	$3.1 \times 10^{10}$	3.0	0.052	0	Direct solution
	2	101	$1.5 \times 10^7$	1.3	.068	0	Multiple heating rate
	3	140	$1.3 \times 10^9$	3.1	.880	0.530	Multiple heating rate
Phenolic II	1	70	$1.3 \times 10^7$	2.0	0.097	0	Integral
	2	122	$5.8 \times 10^8$	2.0	.165	0	Direct solution
	3	172	$7.8 \times 10^{11}$	3.0	.738	0.558	Direct solution
Phenolic III	1	45	$1.3 \times 10^4$	2.0	0.105	0	Direct solution
	2	83	$2.0 \times 10^5$	2.0	.895	0.453	Direct solution
Nylon		232	$5.0 \times 10^{16}$	1.0	1.000	0.070	Direct solution
Silicone		181	$3.2 \times 10^{12}$	1.0	1.000	0.040	Integral
Polyformaldehyde	1	253	$2.5 \times 10^{21}$	1.0	0.190	0	Direct solution
	2	228	$2.4 \times 10^{17}$	1.0	.810	0	Direct solution

## Phenolic I

The small magnitude of the mass-loss rates experienced with phenolic I made it very difficult to obtain rate data from the electronic differentiator. Therefore, a digital computer was used to obtain a least-square fit of a series of polynomials with the TGA data. The mass-loss data as functions of time were divided into five or six overlapping segments and each segment fitted with a polynomial. These polynomials were then differentiated to yield rate data. Figure 3 shows a mass-loss-rate curve as determined in this manner. It can be seen from the peaks and inflections in this curve that at least three mass-loss processes take place. Because of the extensive overlapping of the second and third peaks, the multiple-heating-rate method was applied to these two areas to yield activation energy as a function of mass fraction. Figure 4 shows the activation energy  $E$ , as determined by this method, plotted as a function of the residual mass fraction. By averaging the values of activation energy over the areas of least overlapping, separation of the two reactions was achieved. The averaged values of the kinetic parameters, as determined by the various methods, are shown in table 3. It was found by computing the mass-loss temperature curves from the kinetic parameters in table 3 that reaction 1 was described best by the direct-solution results and reactions 2 and 3 were described best by the multiple-heating-rate results. Figure 5 indicates the precision of fit obtained from these kinetic parameters.

TABLE 3.- AVERAGED VALUES OF KINETIC PARAMETERS FOR PHENOLIC I

Method	Reaction no.	E, kJ/mole	A, min <sup>-1</sup>	n
Direct solution	1	115	$3.1 \times 10^{10}$	3.0
	2	180	$9.1 \times 10^{12}$	3.0
	3	136	$5.1 \times 10^8$	3.0
Integral	1	104	$2.2 \times 10^9$	3.0
	2	155	$1.4 \times 10^{11}$	2.0
	3	166	$1.8 \times 10^{11}$	3.0
Multiple heating rate	1	---	-----	--
	2	101	$1.5 \times 10^7$	1.3
	3	140	$1.3 \times 10^9$	3.1
Difference	1	---	-----	--
	2	74	$1.8 \times 10^2$	1.8
	3	---	-----	--

## Phenolic II

A typical TGA rate plot for phenolic II, presented in figure 6, was derived by a procedure similar to that used for phenolic I. This plot shows the degradation of phenolic II occurring in three steps or reactions. The first step is shown as a broken curve because the absolute magnitude of the rates showed a large amount of variation for the different tests. This variation was due, largely, to the rates being too small to be measured accurately. The broken curve represents only estimated values for these rates. Only the integral method, which does not require rate data, was applied in the first reaction because of this uncertainty in the rate data. The kinetic parameters determined for the first reaction by the integral method are given in table 4. The major part of the

degradation occurs in the two later steps. The direct-solution and difference methods yielded the only consistent results for these two reactions. The kinetic parameters determined for the second and third reactions by these two methods are also given in table 4. The parameters determined by the direct-solution method for the second and third reactions were found to describe the experimental data most accurately. Figure 7 shows a comparison of experimental TGA plots and the TGA plots computed by using these parameters.

TABLE 4.- AVERAGED VALUES OF KINETIC PARAMETERS FOR PHENOLIC II

Method	Reaction no.	E, kJ/mole	A, min <sup>-1</sup>	n
Direct solution	1	---	-----	--
	2	122	$5.8 \times 10^8$	2.0
	3	172	$7.8 \times 10^{11}$	3.0
Integral	1	70	$1.3 \times 10^7$	2.0
	2	---	-----	--
	3	---	-----	--
Difference	1	---	-----	--
	2	64	$3.2 \times 10^1$	2.2
	3	95	$8.6 \times 10^5$	2.0

### Phenolic III

In figure 8 is shown a TGA rate plot determined with the differentiator for phenolic III. Two mass-loss-rate peaks appear in the curve; however, the shape of the second peak indicates that it could be composed of several closely overlapping reactions. Since these reactions could not be resolved, the data were analyzed on the basis of two reactions – a small reaction occurring at low temperatures and a major degradation reaction centered around 770° K. Only the direct-solution and integral methods were applied to these data. Both methods yielded linear Arrhenius plots for  $n = 2.0$  for both reactions, an example of which is shown in figure 9. The kinetic parameters determined by the two methods are presented in table 5. The parameters determined by the direct-solution method give the best fit with experimental data. A comparison of experimental TGA plots and TGA plots computed by using these parameters is shown in figure 10. Except for a region around 720° K, the computed curve compares favorably with the experimental curve. The departure from the experimental curve indicates that the second peak in figure 8 was probably composed of more than one reaction-rate peak.

TABLE 5.- AVERAGED VALUES OF KINETIC PARAMETERS FOR PHENOLIC III

Method	Reaction no.	E, kJ/mole	A, min <sup>-1</sup>	n
Direct solution	1	45	$1.3 \times 10^4$	2.0
	2	83	$2.0 \times 10^5$	2.0
Integral	1	37	$2.4 \times 10^3$	2.0
	2	140	$8.4 \times 10^8$	2.0

### Nylon

The mass-loss-rate curve determined with the differentiator and the TGA plot, as seen in figure 11, indicates that only one major mass-loss reaction occurred in the nylon degradation. The tests of nylon were analyzed by all five methods. The difference

method yielded an average value for the order  $n$  of 1.4 and the multiple-heating-rate method yielded an average value for  $n$  of 1.2. Therefore, the computations by the direct-solution, integral, and maximum-decomposition methods were examined for orders varying between 1.0 and 2.0. It was seen in Arrhenius plots that points compared for  $n = 1.0$  seemed to fit a straight line best. The averaged values of the kinetic parameters  $E$  and  $A$  computed by the integral, direct-solution, and maximum-decomposition methods for  $n = 1.0$  and the averaged values of the kinetic parameters computed by the difference and multiple-heating-rate methods are shown in table 6. The TGA curves computed by using the parameter values in table 6 are compared in figure 12. It can be seen that the results of the different methods yield very different computed curves. A comparison of experimental TGA curves and TGA curves based on parameter values determined from the direct-solution method is shown in figure 13 for three different temperature-rise rates. It can be seen that the values of the kinetic parameters determined by the direct-solution method describe the nylon degradation adequately within this range of heating rates. The activation-energy value used for this plot, 232 kJ/mole, agrees well with a value of 218 kJ/mole reported in reference 6 for nylon 66.

TABLE 6.- AVERAGED VALUES OF KINETIC PARAMETERS FOR NYLON

Method	$E$ , kJ/mole	$A$ , $\text{min}^{-1}$	$n$
Direct solution	232	$5.0 \times 10^{16}$	1.0
Integral	200	$5.0 \times 10^{13}$	1.0
Maximum decomposition	154	$5.0 \times 10^{10}$	1.0
Multiple heating rate	155	$9.4 \times 10^{10}$	1.2
Difference	216	$1.0 \times 10^{14}$	1.4

### Silicone

Mass-loss curves for silicone showed only a single peak. The five methods described herein were used to determine the kinetic parameters of the silicone polymer. The values of these parameters obtained by the various methods are presented in table 7. Computed TGA curves derived from the parameters are shown together with the envelope of experimental data in figure 14. The results of the integral method, maximum-decomposition method, and direct-solution method produced curves close together and within the envelope of experimental data; however, the difference method and the multiple-heating-rate method yielded curves that were way outside of this envelope. It can be seen that any of

TABLE 7.- AVERAGED VALUES OF KINETIC PARAMETERS FOR SILICONE

Method	$E$ , kJ/mole	$A$ , $\text{min}^{-1}$	$n$
Direct solution	150	$2.3 \times 10^{10}$	1.0
Integral	181	$3.2 \times 10^{12}$	1.0
Maximum decomposition	216	$2.8 \times 10^{12}$	1.0
Multiple heating rate	167	$3.6 \times 10^{13}$	1.0
Difference	183	$1.0 \times 10^{14}$	1.37

the three curves within the envelope might be used to describe the wide range of experimental data. This broad range of degradation under similar conditions could be caused by several factors, one of which is slight variations in the effective particle size of the samples. In figure 15 a comparison of TGA plots for a powdered and a solid sample of silicone resin illustrates the effect of extreme variation in effective particle size. This variation is probably due to diffusion effects. Reference 7 reports data for a similar silicone resin whose degradation was diffusion controlled. A random variation in degradation behavior of dimethyl polysiloxane fluids has been reported in reference 8 to be caused by trace impurities catalyzing chain cleavage in the polymer. Therefore, it is also very possible that this mechanism could be contributing to the degradation-range variation experienced in this study. Some of the shift of the mass-loss curve with respect to temperature in figure 15 might be due to changes in temperature calibration. However, no shifts of this magnitude were observed with the other materials.

### Polyformaldehyde

Figure 16 shows a typical TGA mass-loss rate curve for the polyformaldehyde resin obtained by using the differentiator. The direct-solution, integral, and difference methods were applied to the polyformaldehyde data to yield the kinetic parameters in table 8. The parameters determined by the direct-solution method were found to provide the most accurate description of the mass loss. Figure 17 shows a comparison of an experimental TGA plot and a TGA plot computed by using the direct-solution parameters.

TABLE 8.- AVERAGED VALUES OF KINETIC PARAMETERS FOR POLYFORMALDEHYDE

Method	Reaction no.	E, kJ/mole	A, min <sup>-1</sup>	n
Direct solution	1	253	$2.5 \times 10^{21}$	1.0
	2	228	$2.4 \times 10^{17}$	1.0
Integral	1	326	$6.4 \times 10^{26}$	1.0
	2	215	$3.6 \times 10^{16}$	1.0
Difference	1	313	$7.7 \times 10^{26}$	1.0
	2	210	$1.1 \times 10^{16}$	1.0

### Composites

Since the six materials discussed are commonly used in ablative composites, it is desirable that various combinations of these materials be adequately described by the individual sets of parameters. If it is assumed that there is no interaction between the constituent materials, the kinetic parameters determined for each of these materials can be used in equations (24), (25), and (27), developed in appendix B, to describe the mass-loss behavior of a composite material. One such composite of current interest is a mixture (by mass) of 75 percent silicone polymer, 10 percent phenolic II, and 15 percent inert filler. Figure 18 shows a comparison of computed and experimental residual mass fraction as a function of temperature for this composite. The agreement between

experimental and computed data is better for the composite than for the silicone polymer alone, because the composite did not exhibit the variation in behavior that the silicone alone did. In any case, the assumption of no interaction between constituents appears to be a valid one and the mass loss of the composite can be satisfactorily described by the kinetic parameters of its constituents.

Shown in figure 19 is a comparison of computed and experimental TGA plots for a low-density phenolic-nylon. This composite is a mixture (by mass) of 40 percent nylon, 25 percent phenolic I, and 35 percent phenolic II. The agreement is good, as far as curve shape is concerned, even though the temperatures corresponding to the major computed degradation reactions have shifted with respect to those of the experimental plot.

### CONCLUDING REMARKS

The kinetic parameters of six polymeric ablation materials were determined by using the technique of thermogravimetric analysis. The three phenolics and the polyformaldehyde investigated were all found to degrade in two or more sequential mass-loss reactions. Kinetic parameters were determined for each reaction of each material. The nylon was found to degrade in only one mass-loss reaction. The mass-loss behavior of the silicone resin was found to vary randomly from one sample to another. The kinetic parameters determined for each of the six materials appeared to describe the mass-loss behavior, inasmuch as the computed curves provided a close fit with the experimental data.

The parameters for silicone and phenolic II were used to describe the behavior of a phenolic-silicone composite, and these parameters yielded TGA plots in very close agreement with the experimental TGA curves for this composite. The parameters determined for phenolics I and II and for nylon were used to describe the mass-loss behavior of a composite of those materials. The parameters for the phenolic-nylon composite did not describe the mass loss as closely as those for the phenolic-silicone, for they tended to shift the computed curve away from the experimental curve with respect to temperature. However, the curve-shape agreement was good.

It was found that the different methods used to determine the kinetic parameters from TGA data are not equally useful. Direct solution proved to be the most consistently accurate method.

Langley Research Center,  
National Aeronautics and Space Administration,  
Langley Station, Hampton, Va., December 6, 1966,  
129-03-12-03-23.

## APPENDIX A

### METHODS FOR EVALUATING KINETIC PARAMETERS

#### Direct-Solution Method

One of the simplest approaches to evaluating the kinetic parameters in equation (4) is direct solution. By combining equations (1) and (3) and solving for  $k$ , the following equation is obtained:

$$k = \left( \frac{m_0}{m - m_r} \right)^n \left( - \frac{1}{m_0} \frac{dm}{dt} \right) \quad (5)$$

Values of  $k$  can be computed from equation (5) by assuming a value of  $n$  and substituting the values of  $m$  and  $dm/dt$  obtained in the thermogravimetric analysis. By utilizing the values of  $k$  computed from equation (5),  $\ln k$  is plotted as a function of  $1/T$ . If it is assumed that the Arrhenius relation (eq. (2)) holds, the resultant plot should yield a straight line of slope  $-E/R$  and intercept  $\ln A$ . By trying several values of  $n$ , different plots of  $\ln k$  as a function of  $1/T$  are drawn and a value of  $n$  which gives the best fit to the data is selected.

#### Integral Method

In some degradation reactions the mass-loss rates are very small and difficult to determine accurately. For this reason, it is desirable to have a means of determining the kinetic parameters that does not require rate data. Such a method, described in references 9 and 10, is the integral method.

If the temperature-rise rate  $\dot{T}$  is constant, equation (4) may be written as

$$- \frac{\dot{T}}{m_0} \frac{dm}{dT} = \left( \frac{m - m_r}{m_0} \right)^n A e^{-E/RT} \quad (6)$$

It can be noted from equation (4) that as  $T \rightarrow 0$ ,  $dm/dT \rightarrow 0$ ; hence,  $m_{T=0} = m_0$ .

The variables of equation (6) can be separated to form the integrals

$$- \frac{1}{m_0} \int_{m_0}^m \left( \frac{m - m_r}{m_0} \right)^{-n} dm = \frac{A}{\dot{T}} \int_0^T e^{-E/RT} dT = K \quad (7)$$

where  $K$  is termed the integral parameter.

## APPENDIX A

The first integral in equation (7) gives

$$K = -\ln\left(\frac{m - m_r}{m_o - m_r}\right) \quad (8)$$

for  $n = 1$  and

$$K = (n - 1)^{-1} \left[ \left(\frac{m - m_r}{m_o}\right)^{1-n} - \left(1 - \frac{m_r}{m_o}\right)^{1-n} \right] \quad (9)$$

for  $n \neq 1$ .

The second integral in equation (7) may be expressed as

$$K = \frac{AE}{RT} p(X) \quad (10)$$

where

$$\left. \begin{aligned} p(X) &= \frac{e^{-X}}{X} - [-\text{Ei}(-X)] \\ X &= \frac{E}{RT} \end{aligned} \right\} \quad (11)$$

The term  $-\text{Ei}(-X)$  is the exponential integral. By using an asymptotic expansion for  $-\text{Ei}(-X)$ , equation (10) can be written as

$$K = \frac{AE}{RT} \left( 1 - \frac{2!}{X} + \frac{3!}{X^2} - \frac{4!}{X^3} + \dots \right) X^{-2} e^{-X} \quad (12)$$

If the first term of the series is defined as

$$q(X) = X^{-2} e^{-X} \quad (13)$$

then  $K$  may be expressed as

$$K = r \frac{AE}{RT} q(X) \quad (14)$$



## APPENDIX A

where

$$r = \frac{p(X)}{q(X)} \quad (15)$$

The term  $(1 - r)$  is the relative error associated with using only the first term of the series. A plot of  $(1 - r)$  as a function of  $X$  is shown in figure 20. It can be noted that  $r$  is a slowly varying function of  $X$  for  $X > 20$ , the range of primary interest for the materials considered herein. Combining equations (13) and (14) yields

$$\frac{K}{T^2} = r \frac{AR}{E\dot{T}} e^{-E/RT} \quad (16)$$

From the TGA data and assumed values of  $n$ , equations (8) and (9) may be used to obtain  $K$ . Inasmuch as  $r$  is nearly constant with respect to  $E/RT$ , a plot of  $\ln \frac{K}{T^2}$  as a function of  $1/T$  would be nearly linear. As in the direct-solution method,  $E$  may be calculated from the slope and  $A$  from the intercept.

### Method of Maximum Decomposition

A rapid method of evaluating the kinetic parameters, based on the point of maximum decomposition rate, has been reported in reference 11.

Putting equation (6) into the form

$$-\frac{dm}{dT} = \frac{m_o}{\dot{T}} \left( \frac{m - m_r}{m_o} \right)^n A e^{-E/RT}$$

and maximizing the rate  $dm/dT$  yield

$$\frac{d}{dT} \left( -\frac{dm}{dT} \right) = \frac{-m_o A e^{-E/RT}}{\dot{T}} \left[ - \left( \frac{m_m - m_r}{m_o} \right)^n \frac{E}{RT_m^2} + n \left( \frac{m_m - m_r}{m_o} \right)^{n-1} \frac{1}{m_o} \left( \frac{dm}{dT} \right)_{\max} \right] = 0 \quad (17)$$

where  $m_m$  is the mass at maximum rate of mass loss,  $T_m$  is the temperature at maximum rate of mass loss, and  $\left( \frac{dm}{dT} \right)_{\max}$  is the maximum rate of mass loss.

Simplifying equation (17) yields

$$E = \frac{nRT_m^2 \left( \frac{dm}{dT} \right)_{\max}}{m_m - m_r} \quad (18)$$

## APPENDIX A

By using equation (18), the activation energy can be evaluated for an assumed value of  $n$  at the maximum point of the TGA rate curve. The frequency factor can be solved from the rate equation (eq. (4)) written as

$$A = - \frac{dm}{dt} \left( \frac{m_o}{m - m_r} \right)^n e^{E/RT} \quad (19)$$

### Multiple-Heating-Rate Method

Another interesting method has been reported in reference 11. This method requires several tests at different heating rates, but determines all three kinetic parameters –  $E$ ,  $A$ , and  $n$ .

Equations (1) and (2) are combined and the logarithm is taken to yield:

$$\ln \left( - \frac{1}{m_o} \frac{dm}{dt} \right) = \ln \left[ Af \left( \frac{m}{m_o} \right) \right] - \frac{E}{RT} \quad (20)$$

By performing several tests at different heating rates and taking values of  $dm/dt$  and  $T$  at constant values of  $m/m_o$  from each test,  $\ln \left( - \frac{1}{m_o} \frac{dm}{dt} \right)$  can be plotted as a function of  $1/T$  for each chosen value of  $m/m_o$ . The slope of each line is equal to  $-E/R$ . This method gives  $E$  as a function of  $m/m_o$  without assuming any form for  $f(m/m_o)$ . The order  $n$  and the frequency factor  $A$  can be found after deciding what form  $f(m/m_o)$  must take. The form used herein was that of equation (3), which is

$$f \left( \frac{m}{m_o} \right) = \left( \frac{m - m_r}{m_o} \right)^n$$

If  $\ln \left[ Af \left( \frac{m}{m_o} \right) \right]$  is plotted as a function of  $\ln \left( \frac{m - m_r}{m_o} \right)$ , the slope is equal to the order and the frequency factor is determined from the intercept.

### Difference Method

A number of methods reported in the literature (see refs. 9, 12, and 13) are based on a difference method applied to some form of the rate equation. The variation reported herein is a modification of the method in reference 13 and is described in detail in reference 12.

## APPENDIX A

This method uses the rate expression

$$-\frac{dm}{dt} = (m - m_r)^n A e^{-E/RT} \quad (21)$$

which is similar to equation (4).

Putting equation (21) into logarithmic form and taking finite differences give

$$\Delta \ln \left( -\frac{dm}{dt} \right) = n \Delta \ln(m - m_r) - \frac{E}{R} \Delta \frac{1}{T} \quad (22)$$

If values for  $\Delta \ln \left( -\frac{dm}{dt} \right)$  and  $\Delta \ln(m - m_r)$  are found for a constant increment  $\Delta \frac{1}{T}$ ,  $\Delta \ln \left( -\frac{dm}{dt} \right)$  can be plotted as a function of  $\Delta \ln(m - m_r)$ . This plot should be a straight line, the slope of which is equal to the reaction order  $n$ . The activation energy  $E$  may be computed from the intercept. With both  $n$  and  $E$  known, the frequency factor  $A$  can be solved from equation (21).

This method, like the multiple-heating-rate method, has the advantage of determining all three kinetic parameters. In practice, the usefulness of the difference method is limited because of its sensitivity to small errors in the experimental data and the resulting large amount of data scatter (ref. 9). This scatter can be minimized by choosing an optimum increment for  $1/T$ .

## APPENDIX B

### DEVELOPMENT OF EQUATIONS USED IN COMPUTING THERMOGRAVIMETRIC PLOTS

Determining the kinetic parameters by more than one method provides a check on the validity of these parameters. However, a better check is a comparison between an actual TGA plot and one computed from the calculated kinetic parameters. An integrated form of the rate equation (eq. (4)) is necessary to compute a TGA plot. The integral method in appendix A provides a convenient integrated form of the rate equation. From equations (8) and (16),

$$-\ln\left(\frac{m - m_r}{m_o - m_r}\right) = r \frac{AR}{E\dot{T}} T^2 e^{-E/RT} \quad (23)$$

for  $n = 1$ .

If  $r \approx 1$ , equation (23) may be solved for  $m/m_o$  to yield

$$\frac{m}{m_o} = \frac{m_r}{m_o} + \frac{m_o - m_r}{m_o} \exp\left(\frac{-AT^2}{\dot{T} \frac{E}{R}} e^{-E/RT}\right) \quad (24)$$

for  $n = 1$ .

Similarly, from equations (9) and (16),

$$\frac{m}{m_o} = \frac{m_r}{m_o} + \left[ \left( \frac{m_o - m_r}{m_o} \right)^{1-n} + \frac{(n-1)AT^2}{\dot{T} \frac{E}{R}} e^{-E/RT} \right]^{\frac{1}{1-n}} \quad (25)$$

for  $n \neq 1$ .

Often, more than one reaction takes place. For example, a single material may have several distinct mass-loss reactions or a composite material of several polymers may have one or more reactions for each polymer.

Therefore, for the case of no interactions, a multiple-reaction mass balance can be written as

$$\frac{m}{m_o} = \frac{m_1}{m_o} + \frac{m_2}{m_o} + \dots + \frac{m_i}{m_o} \quad (26)$$

## APPENDIX B

where  $m$  is the total mass of sample at temperature  $T$ ,  $m_i$  is the mass of material in reaction  $i$  at temperature  $T$ , and  $m_o$  is the total original mass.

Equation (26) can be written in the form

$$\frac{m}{m_o} = \frac{m_{o,1}}{m_o} \frac{m_1}{m_{o,1}} + \frac{m_{o,2}}{m_o} \frac{m_2}{m_{o,2}} + \dots + \frac{m_{o,i}}{m_o} \frac{m_i}{m_{o,i}} \quad (27)$$

where  $m_{o,i}$  is the original mass of material in reaction  $i$  and  $m_i/m_{o,i}$  is described by equations (24) and (25) for each constituent.

In this way, the mass-loss behavior of a large number of composites may be described, if the kinetic parameters and the relative proportions of the constituent materials are known.

## REFERENCES

1. Swann, Robert T.; Pittman, Claud M.; and Smith, James C.: One-Dimensional Numerical Analysis of the Transient Response of Thermal Protection Systems. NASA TN D-2976, 1965.
2. Beecher, Norman; and Rosensweig, Ronald E.: Ablation Mechanisms in Plastics With Inorganic Reinforcement. ARS J., vol. 31, no. 4, Apr. 1961, pp. 532-539.
3. Mechtly, E. A.: The International System of Units - Physical Constants and Conversion Factors. NASA SP-7012, 1964.
4. Müller, Ralph H.: Automatic Recording Vacuum Thermobalance Records Weight Changes as Function of Temperature or Time. Anal. Chem., vol. 32, no. 1, Jan. 1960, pp. 77 A - 77 B.
5. Freeman, G. G.: Silicones. Iliffe Books Ltd. (London), 1962.
6. Kratsch, K. M.; Hearne, L. F.; and McChesney, H. R.: Thermal Performance of Heat Shield Composites During Planetary Entry. Presented at AIAA-NASA National Meeting (Palo Alto, Calif.), Sept. 30-Oct. 1, 1963.
7. Doyle, Charles D.: Logarithmic Thermal Degradation of a Silicone Resin in Air. J. Polymer Sci., vol. XXXI, no. 122, Aug. 1958, pp. 95-104.
8. Lewis, Charles W.: The Pyrolysis of Dimethylpolysiloxanes. II. J. Polymer Sci., vol. XXXVII, no. 132, June 1959, pp. 425-429.
9. Farmer, Rex W.: Thermogravimetry of Plastics - Part I: Empirical Homogeneous Kinetics. ASD-TDR-62-1043; Pt. I, U.S. Air Force, Feb. 1963.
10. Doyle, Charles D.: Evaluation of Experimental Polymers. WADD Tech. Rept. 60-283, U. S. Air Force, June 1960 (Available from ASTIA as AD No. 243387-L.)
11. Friedman, Henry L.: The Kinetics of Thermal Degradation of Charring Plastics. I. Glass Reinforced Phenol-Formaldehyde. R61SD145 (Contract No. AF 04(647)-269), Missile and Space Div., Gen. Elec. Co., Aug. 1961.
12. Anderson, David A.; and Freeman, Eli S.: The Kinetics of the Thermal Degradation of Polystyrene and Polyethylene. J. Polymer Sci., vol. 54, no. 159, Sept. 1961, pp. 253-260.
13. Freeman, Eli S.; and Carroll, Benjamin: The Application of Thermoanalytical Techniques to Reaction Kinetics. The Thermogravimetric Evaluation of the Kinetics of the Decomposition of Calcium Oxalate Monohydrate. J. Phys. Chem., vol. 62, no. 4, Apr. 1958, pp. 394-397.

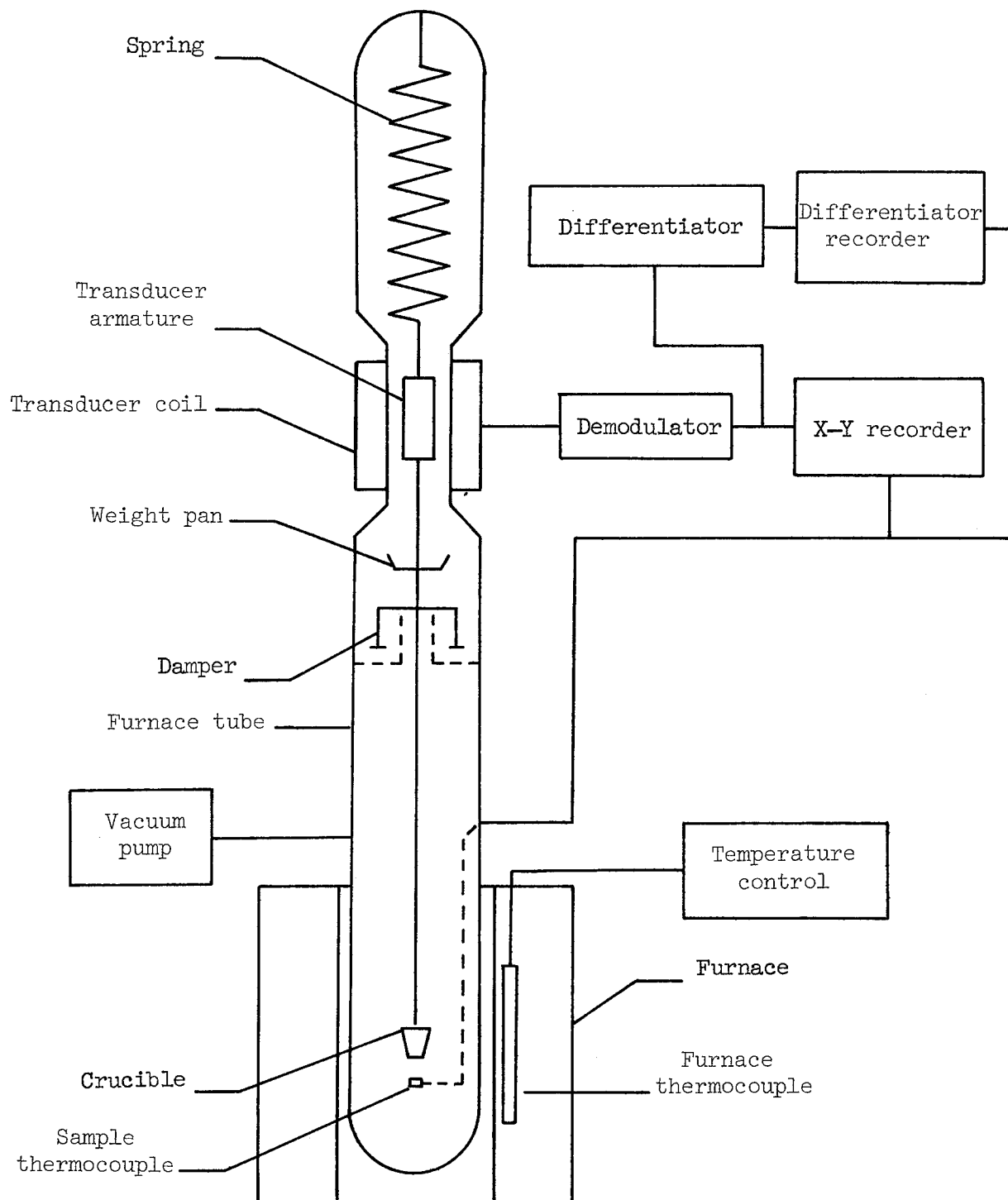


Figure 1.- Schematic of apparatus.

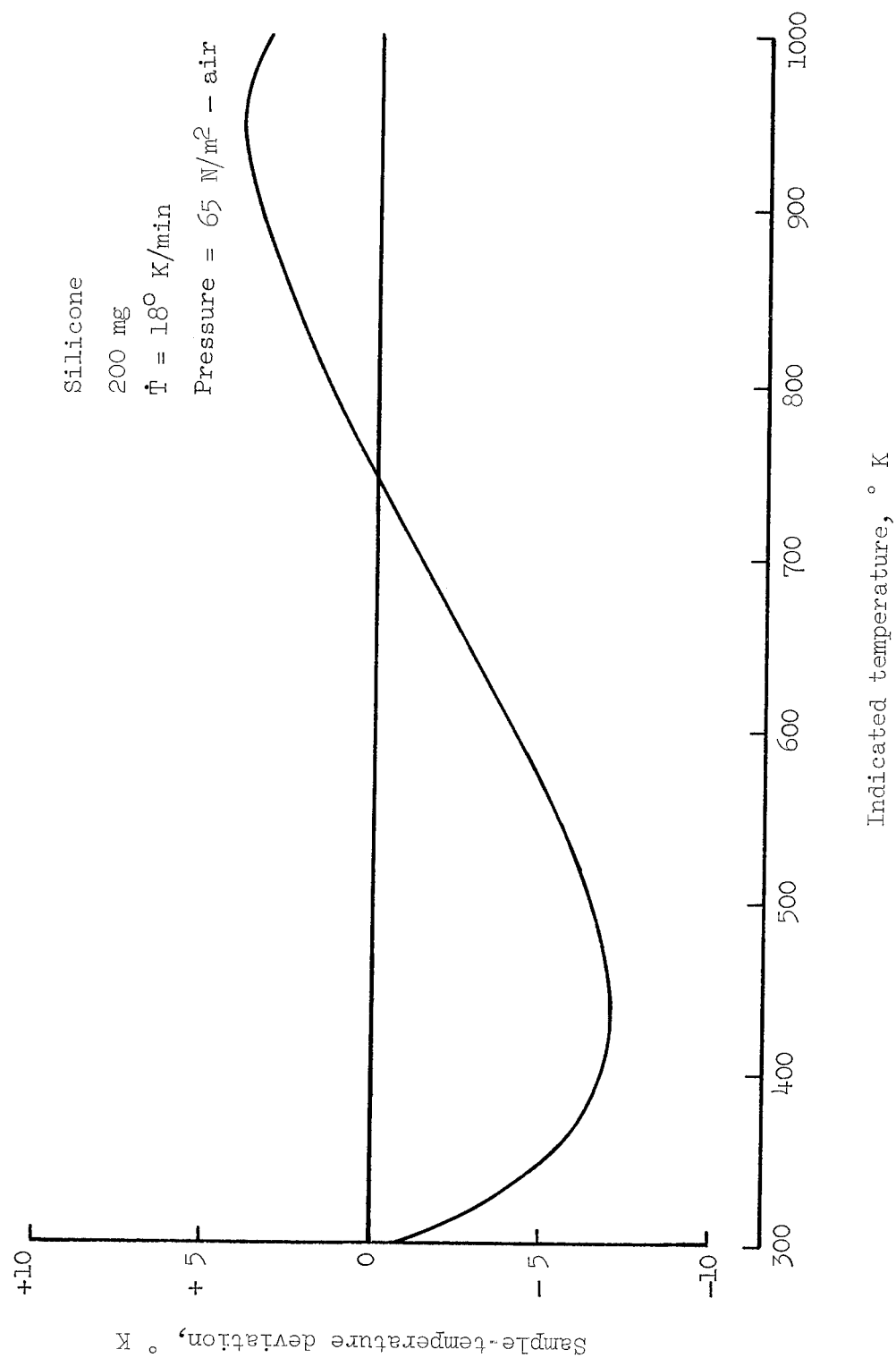


Figure 2.- Typical example of the deviation of sample temperature from the indicated temperature.



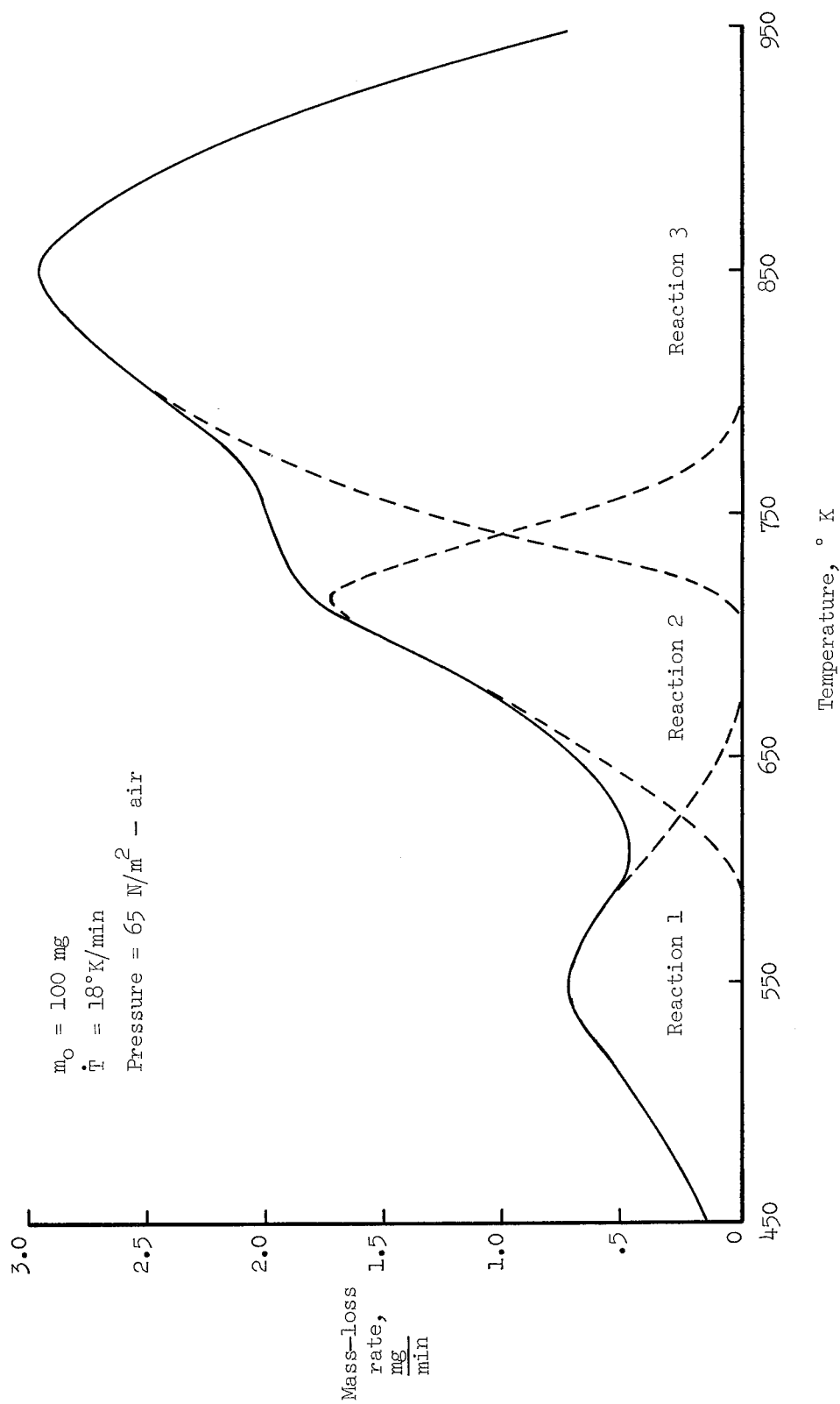


Figure 3.- Mass-loss-rate curve for phenolic I.

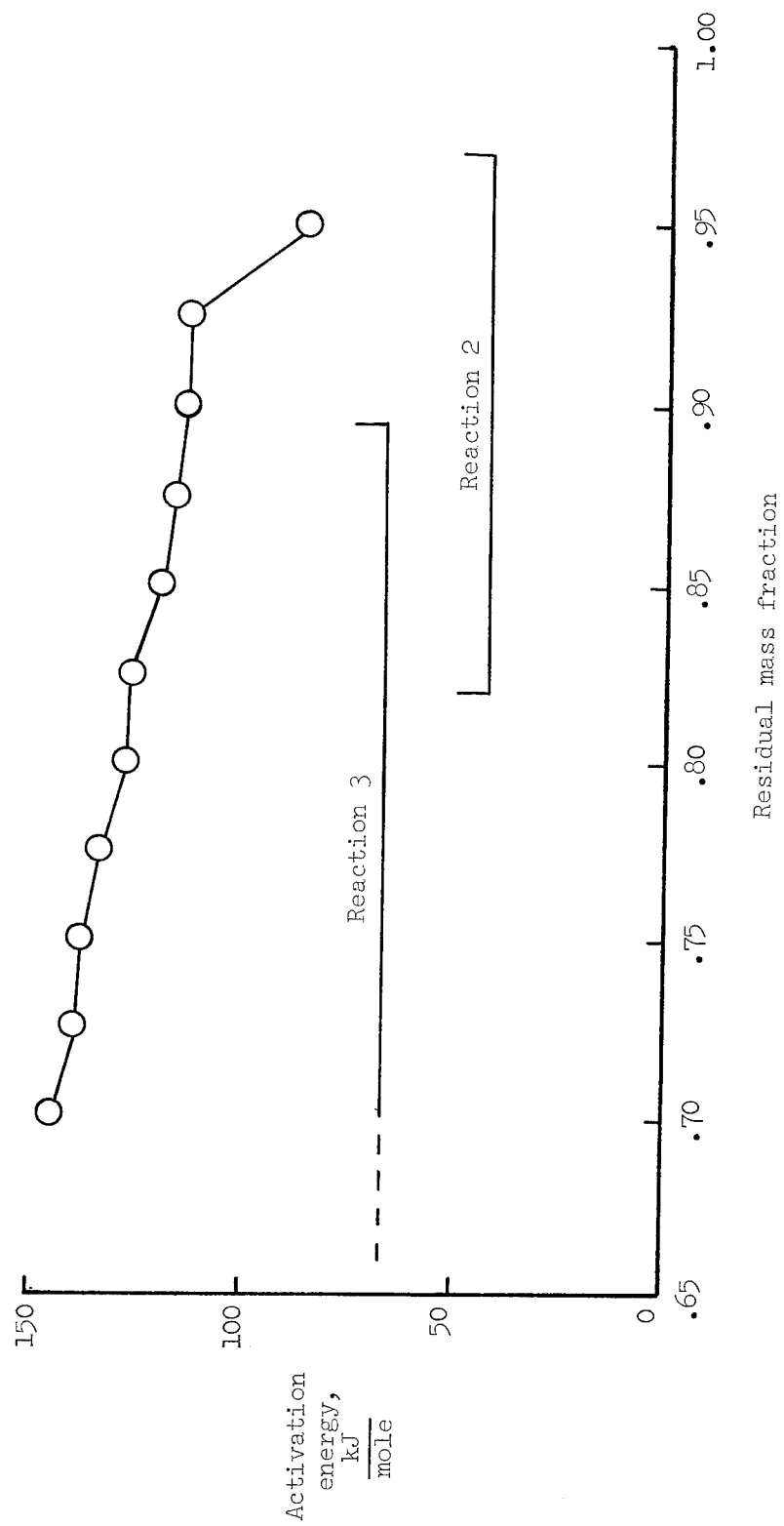


Figure 4.- Activation energy as a function of mass fraction for phenolic I.

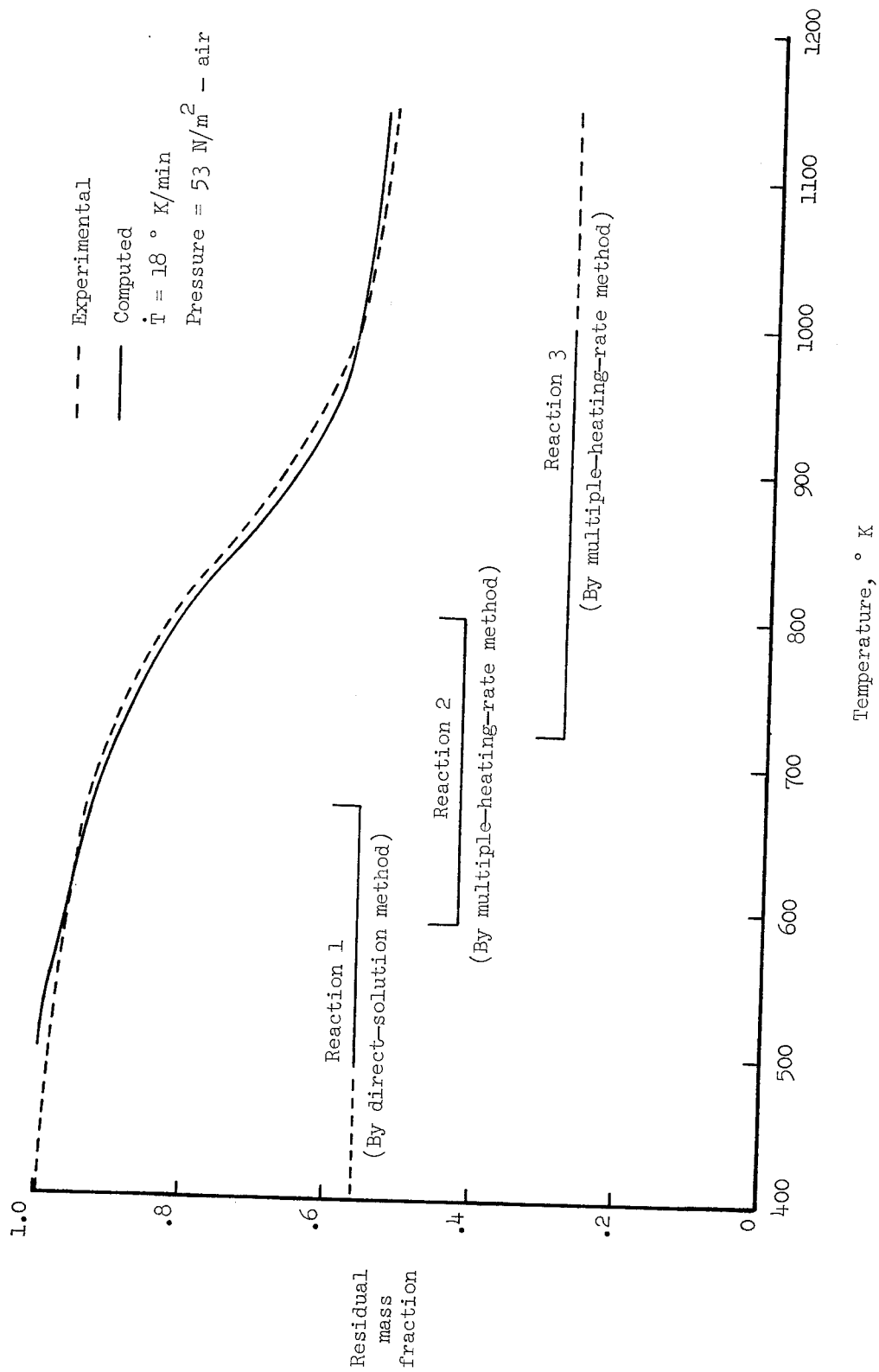


Figure 5.- Experimental and computed TGA plots for phenolic I.

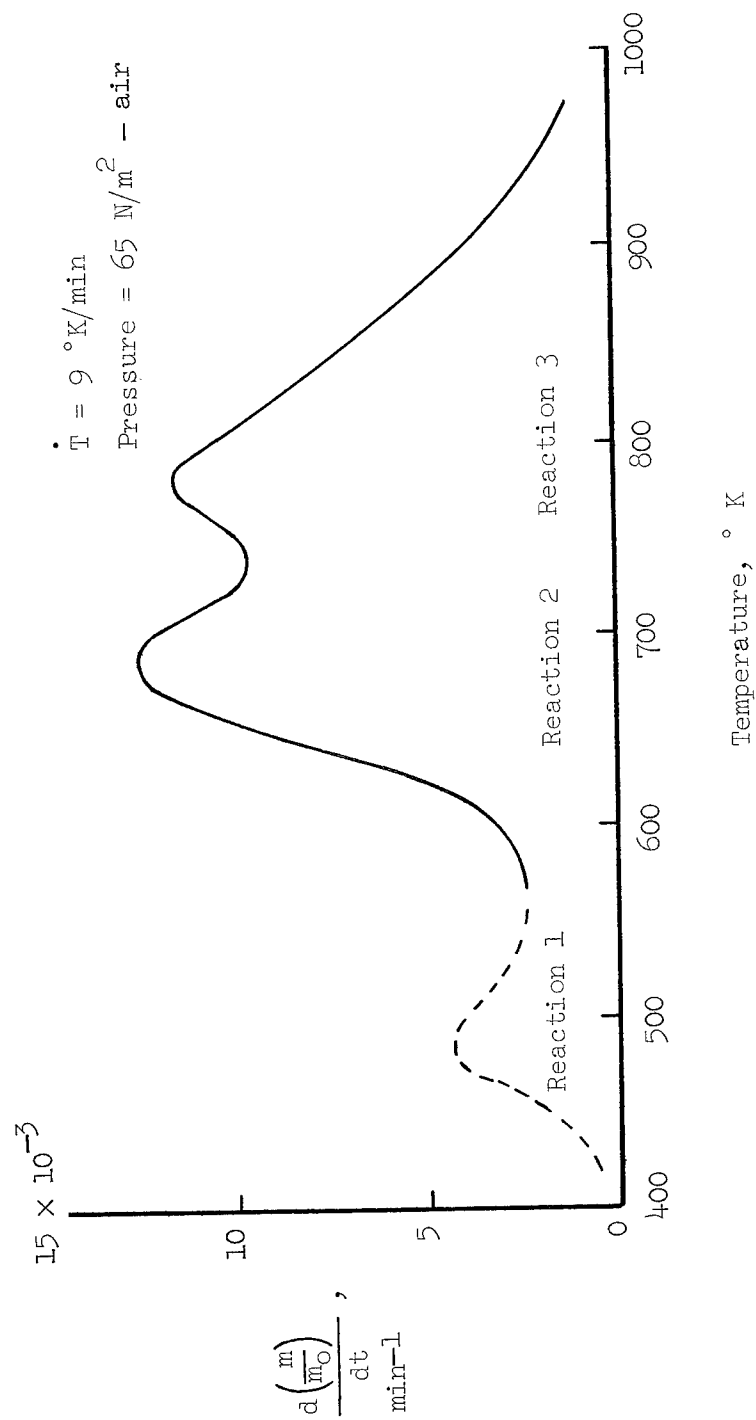


Figure 6.- TGA rate plot for phenolic II.

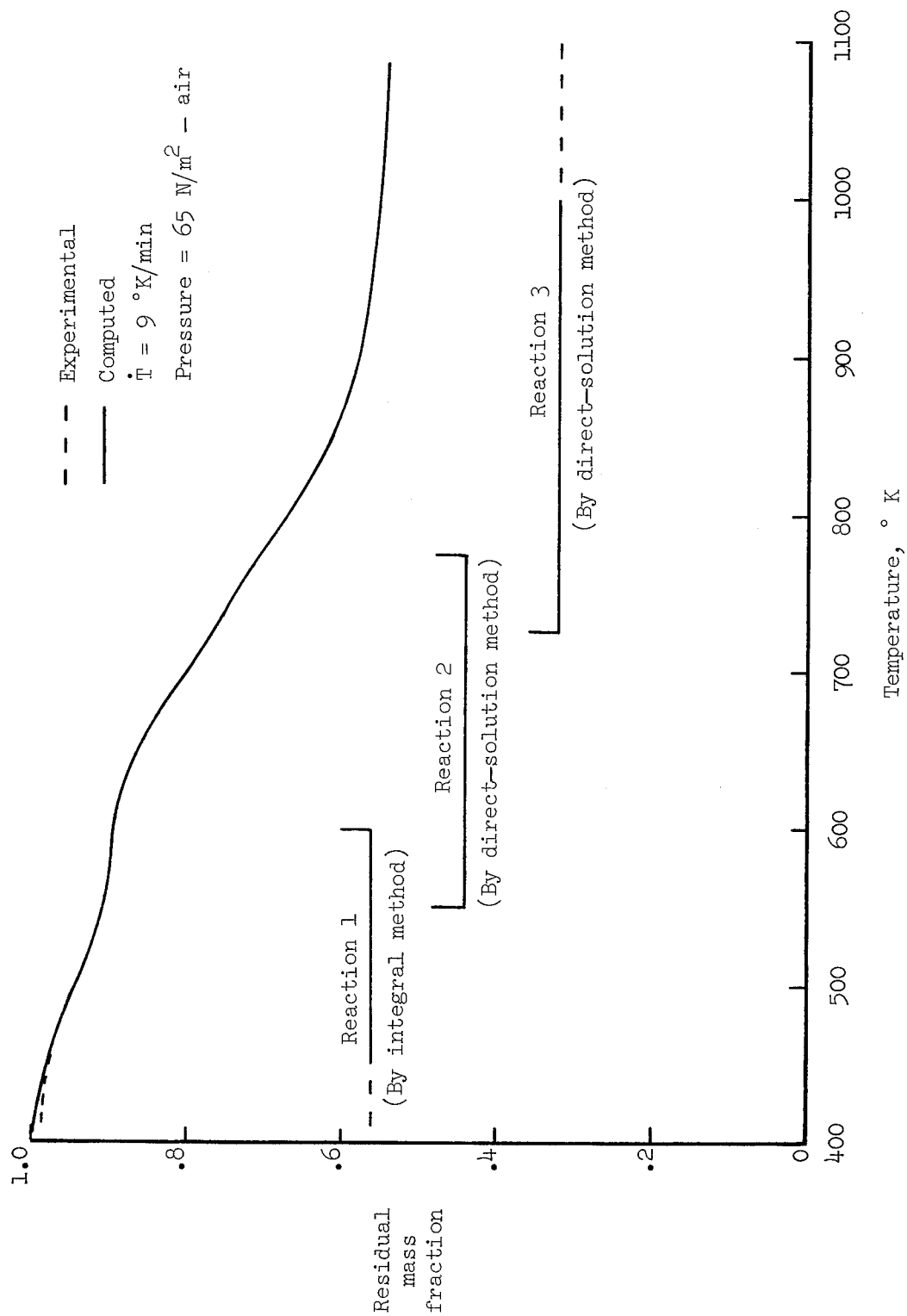


Figure 7.- Experimental and computed TGA plots for phenolic II.

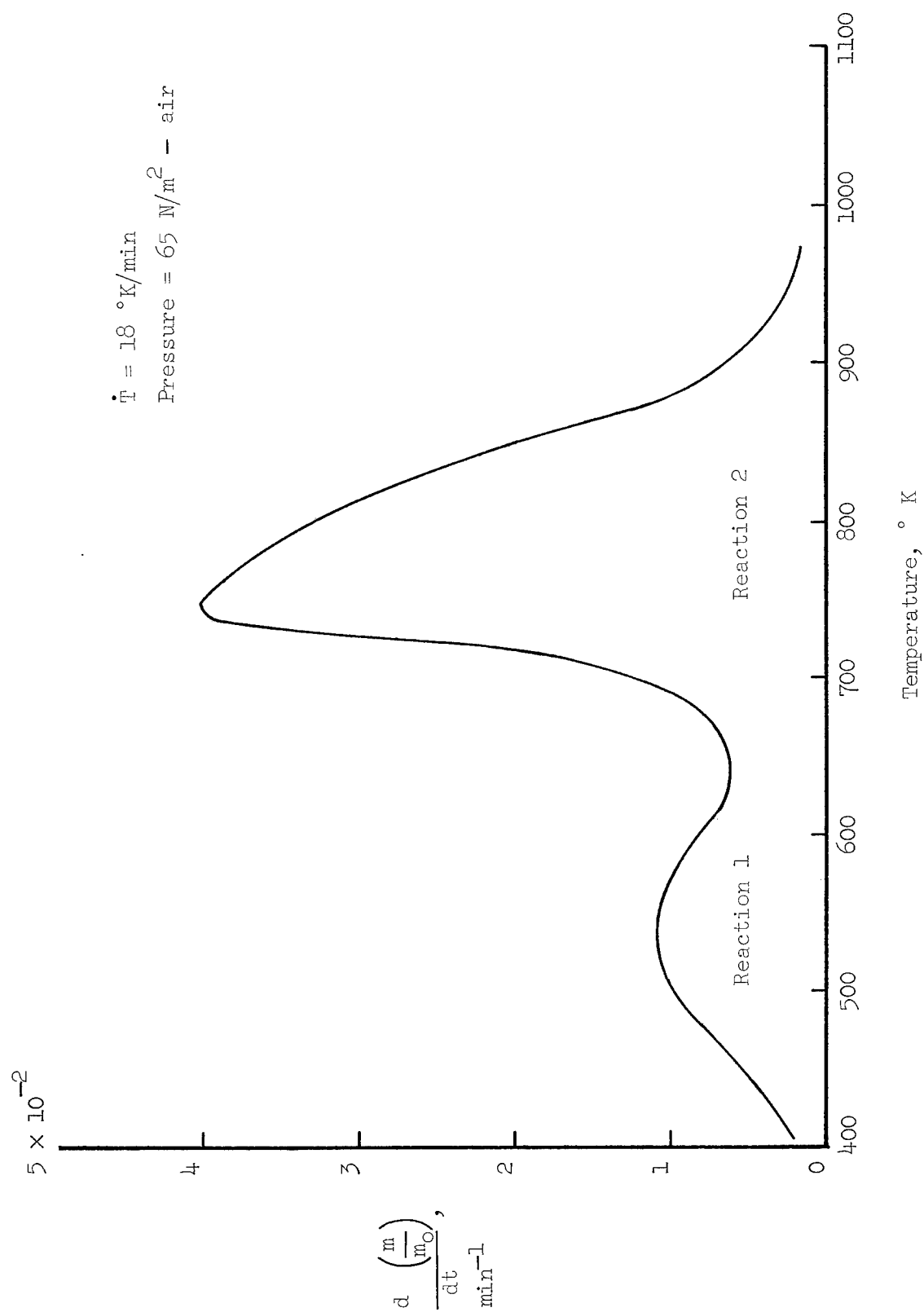


Figure 8.- TGA rate plot for phenolic III.

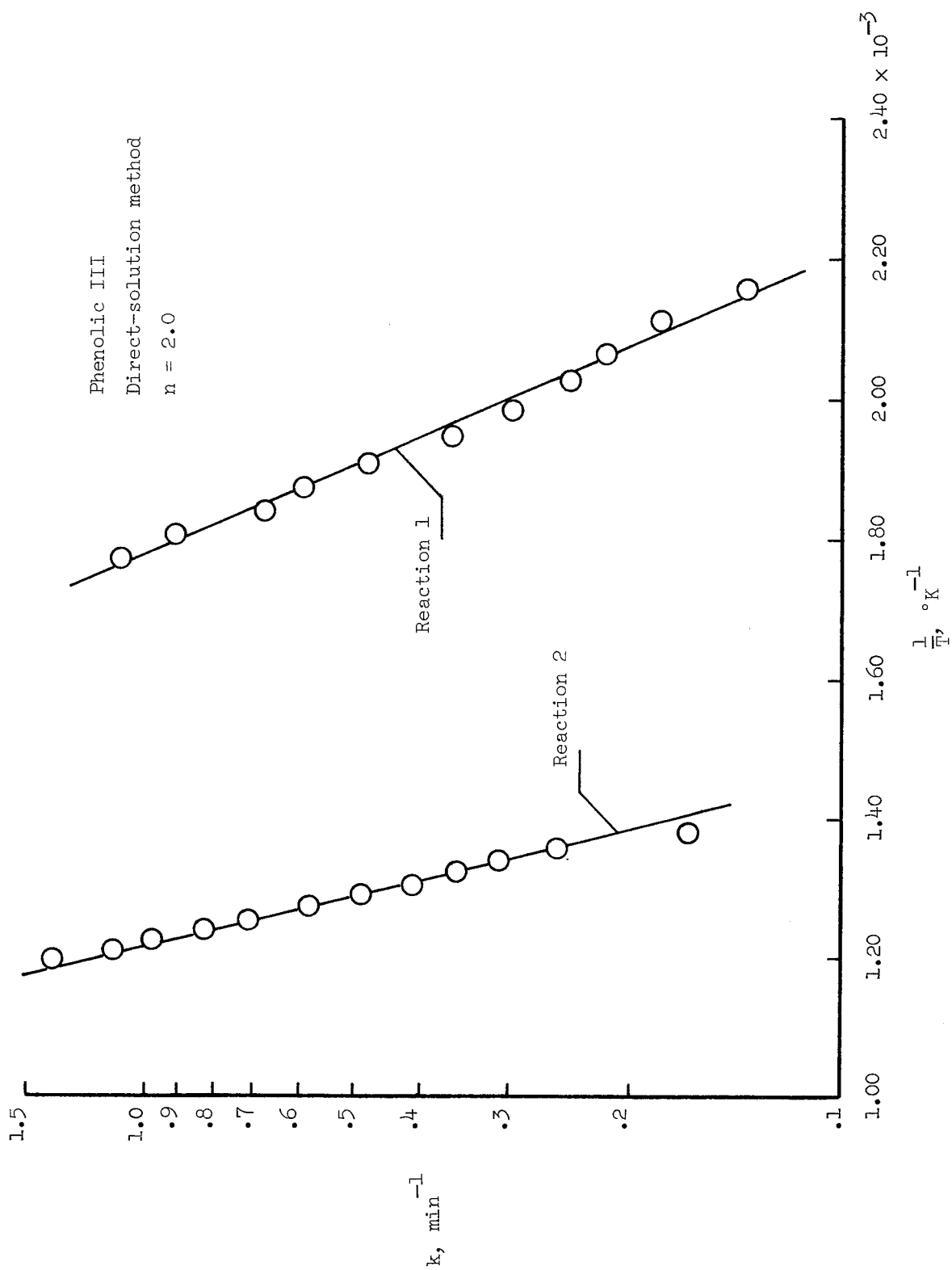


Figure 9.- Arrhenius plots for phenolic III.

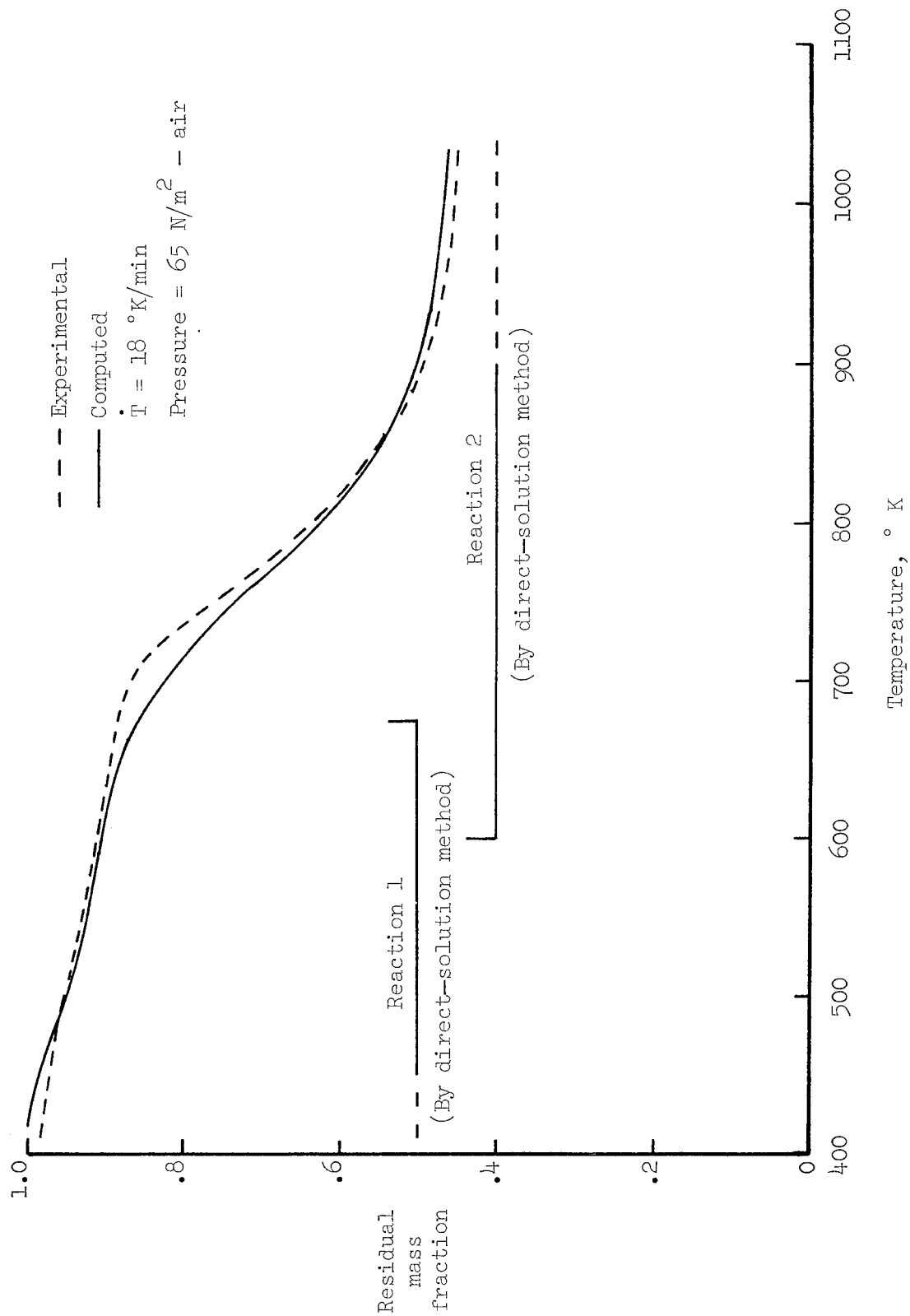


Figure 10.- Experimental and computed TGA plots for phenolic III.



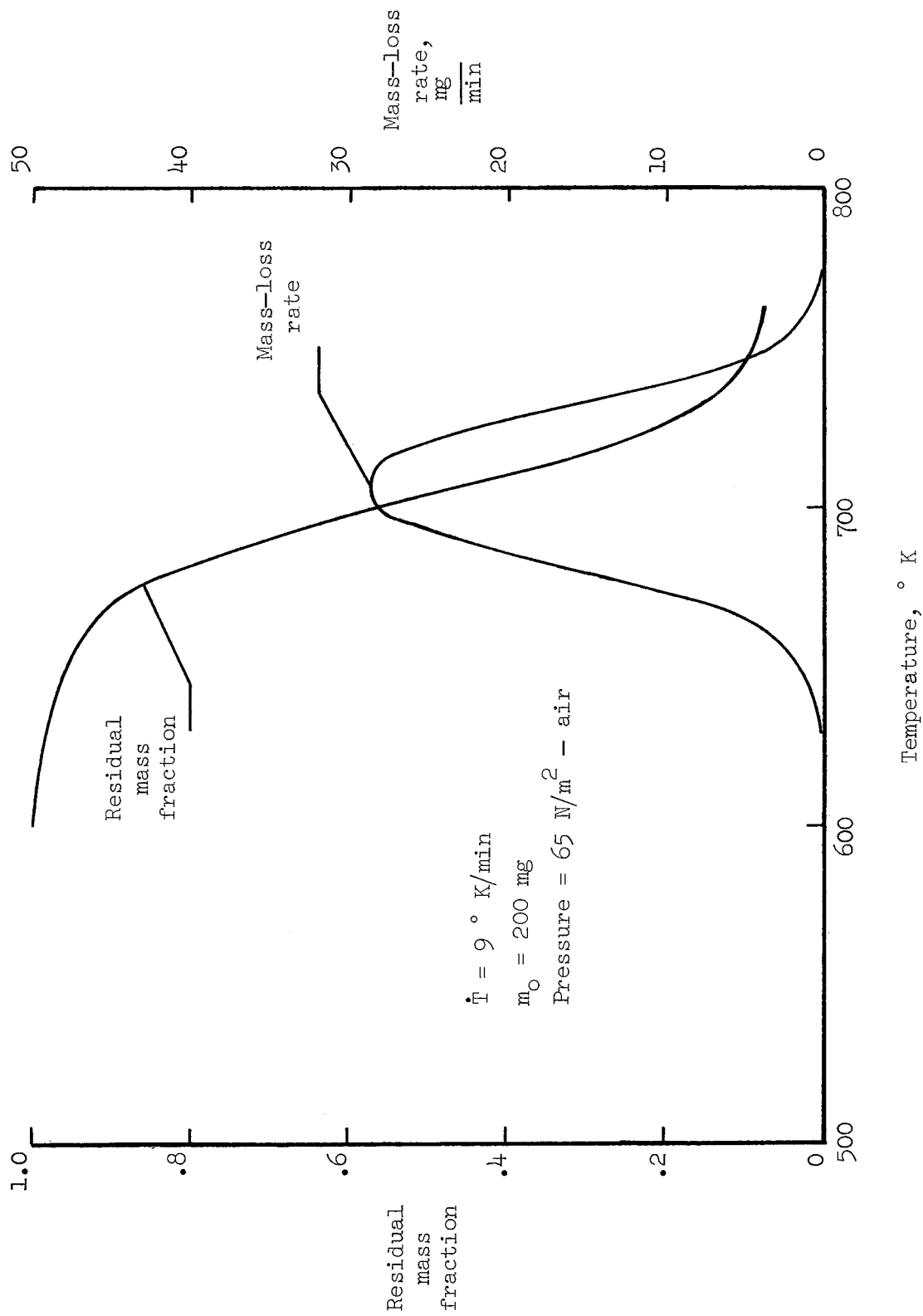


Figure 11.- Residual mass fraction and mass-loss rate for nylon.

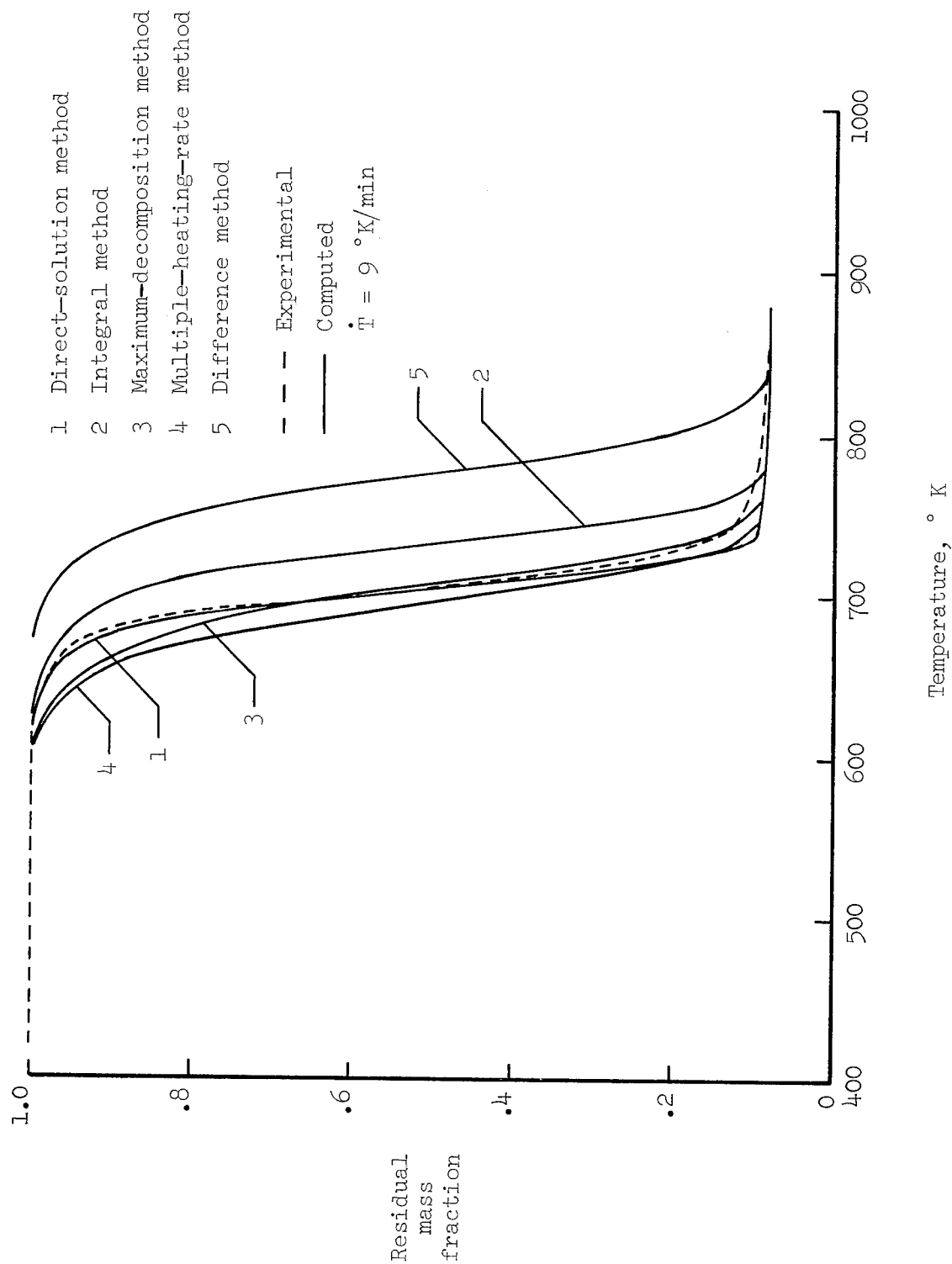


Figure 12.- Experimental and computed TGA plots for nylon.

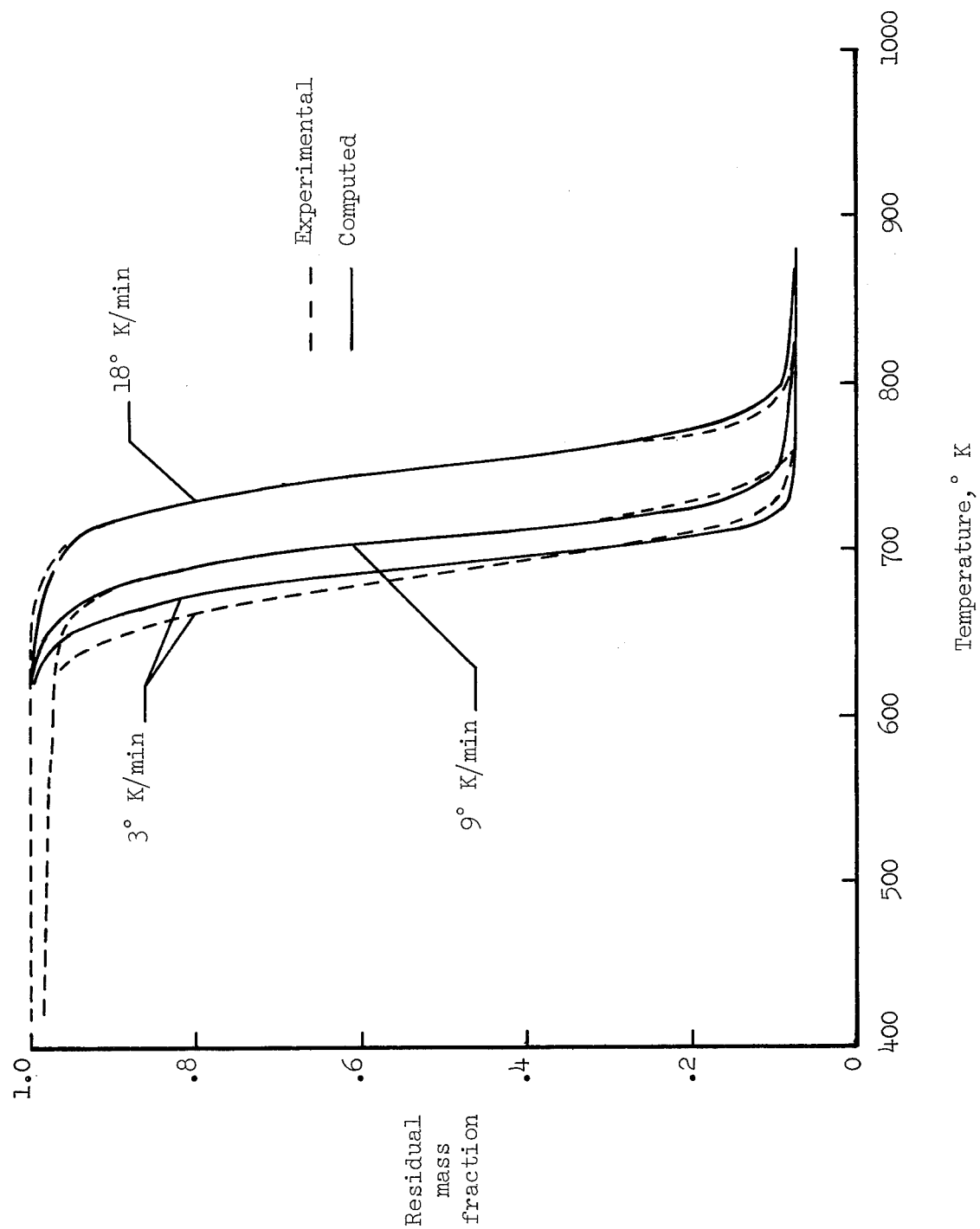


Figure 13.- Experimental TGA plots and computed TGA plots, obtained by using the direct-solution method, for nylon at different temperature-rise rates.  
 $E = 232 \text{ kJ/mole.}$

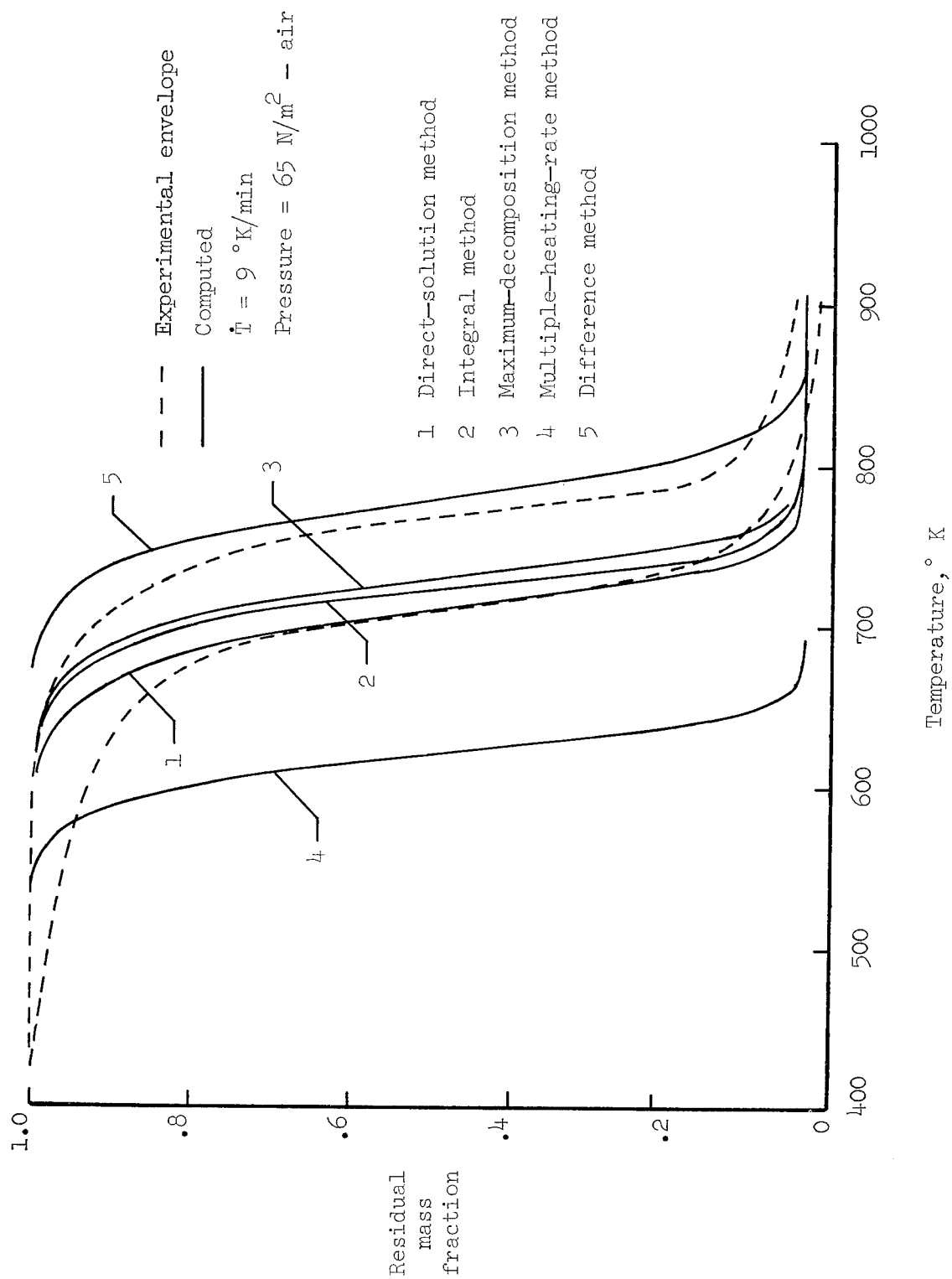


Figure 14.- Experimental and computed TGA plots for silicone.

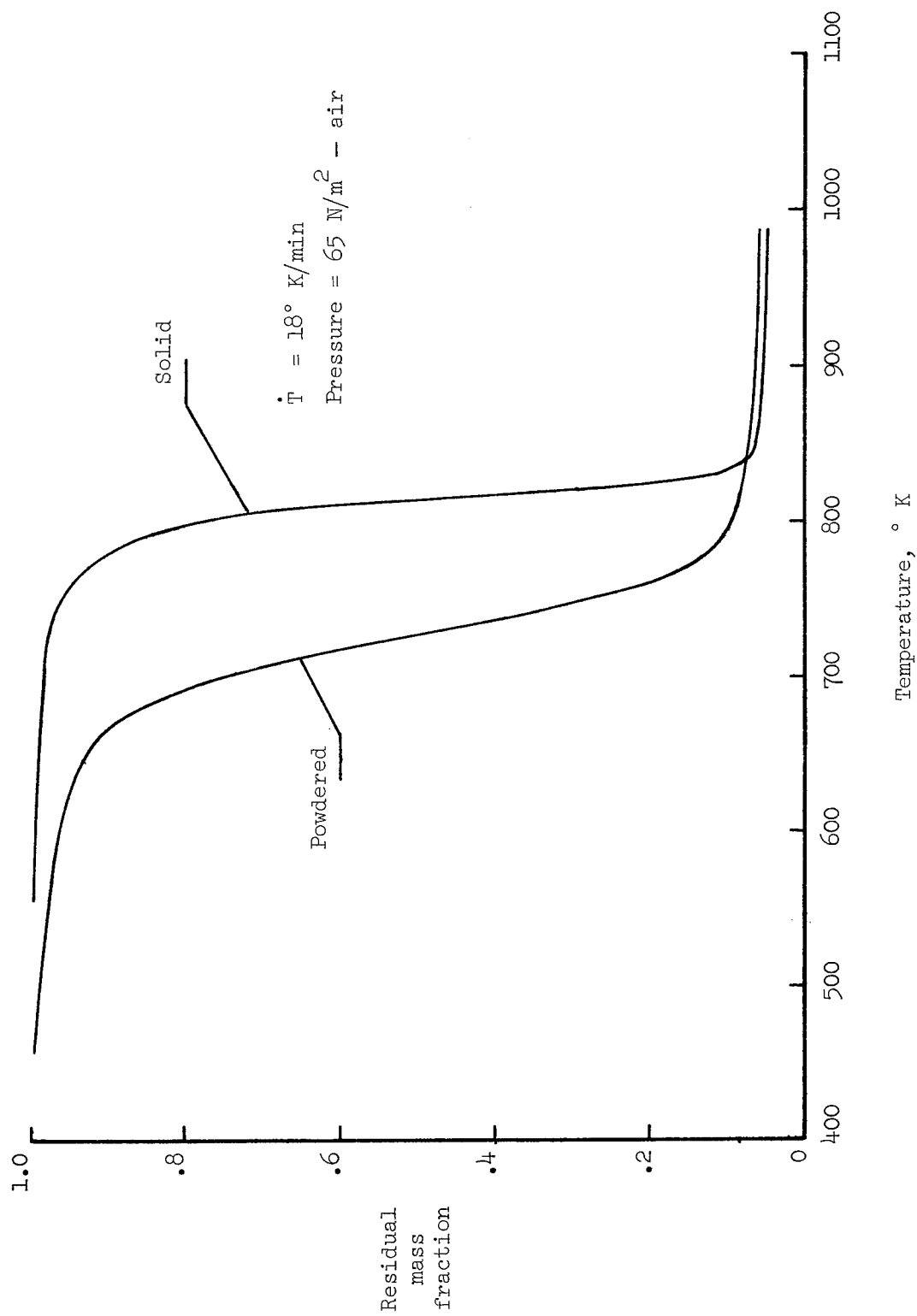


Figure 15.- Comparison of TGA plots for solid and powdered silicone.

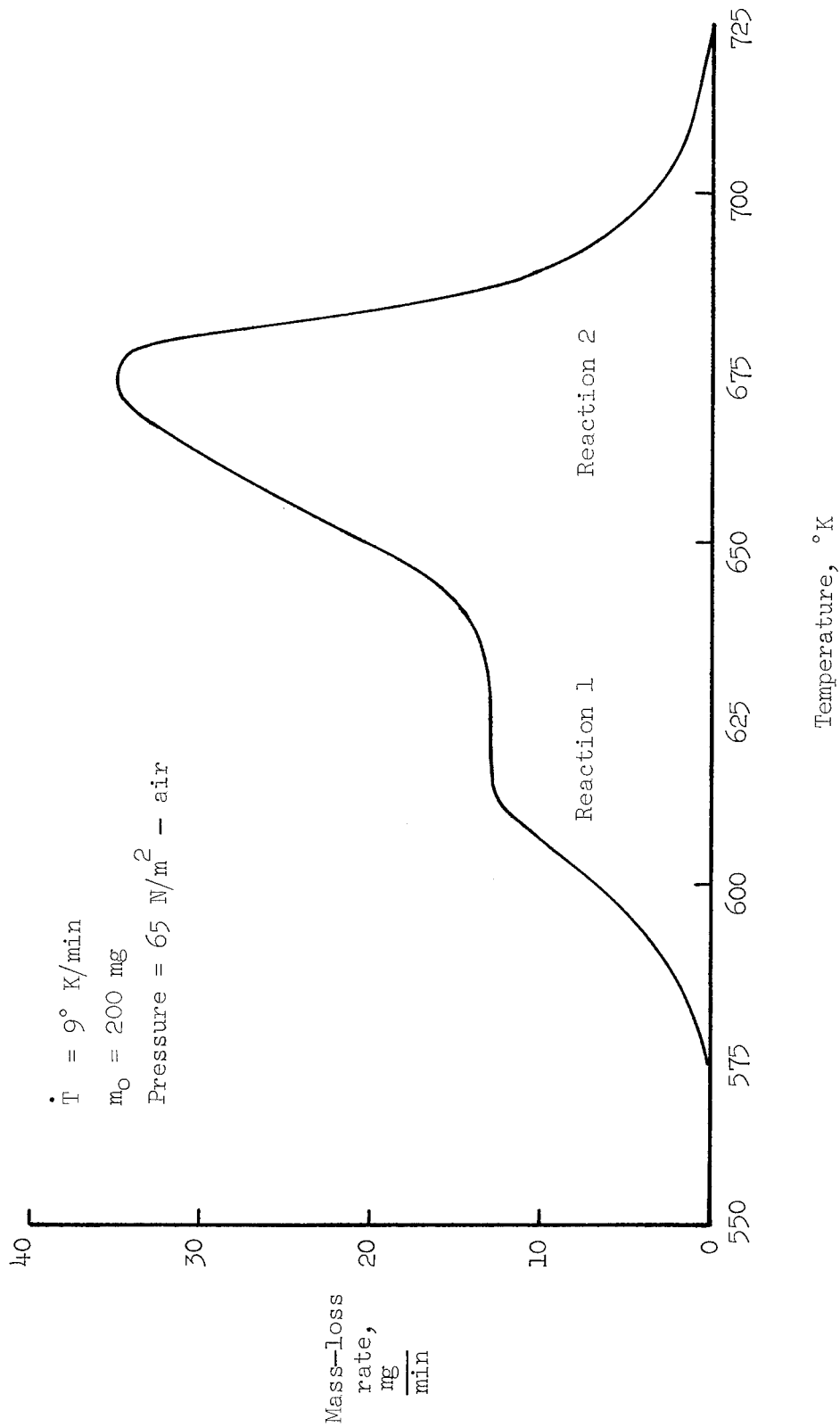


Figure 16.- Mass-loss-rate curve for polyformaldehyde.

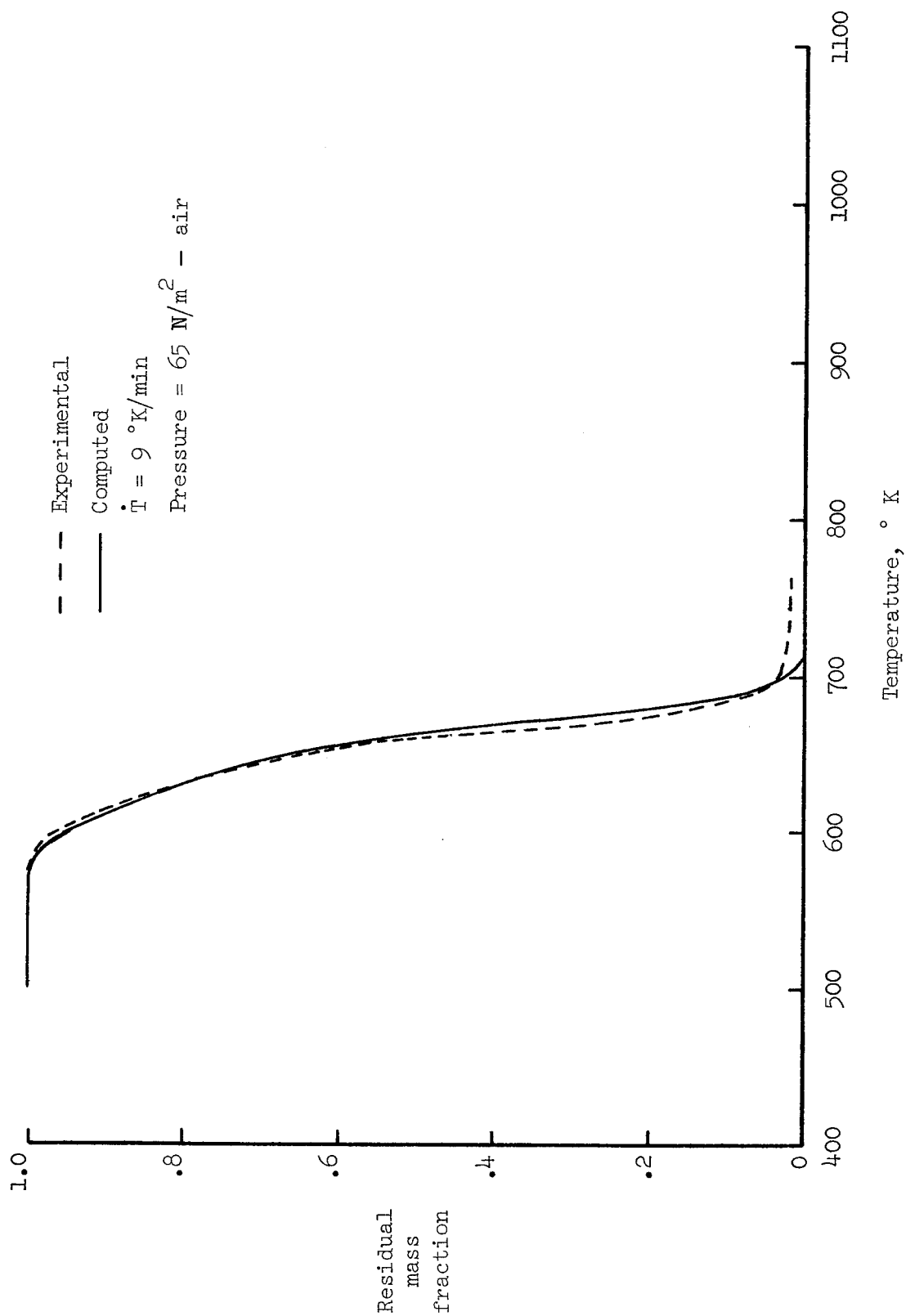


Figure 17.- An experimental TGA plot and a computed TGA plot, obtained by using the direct-solution method, for polyformaldehyde.

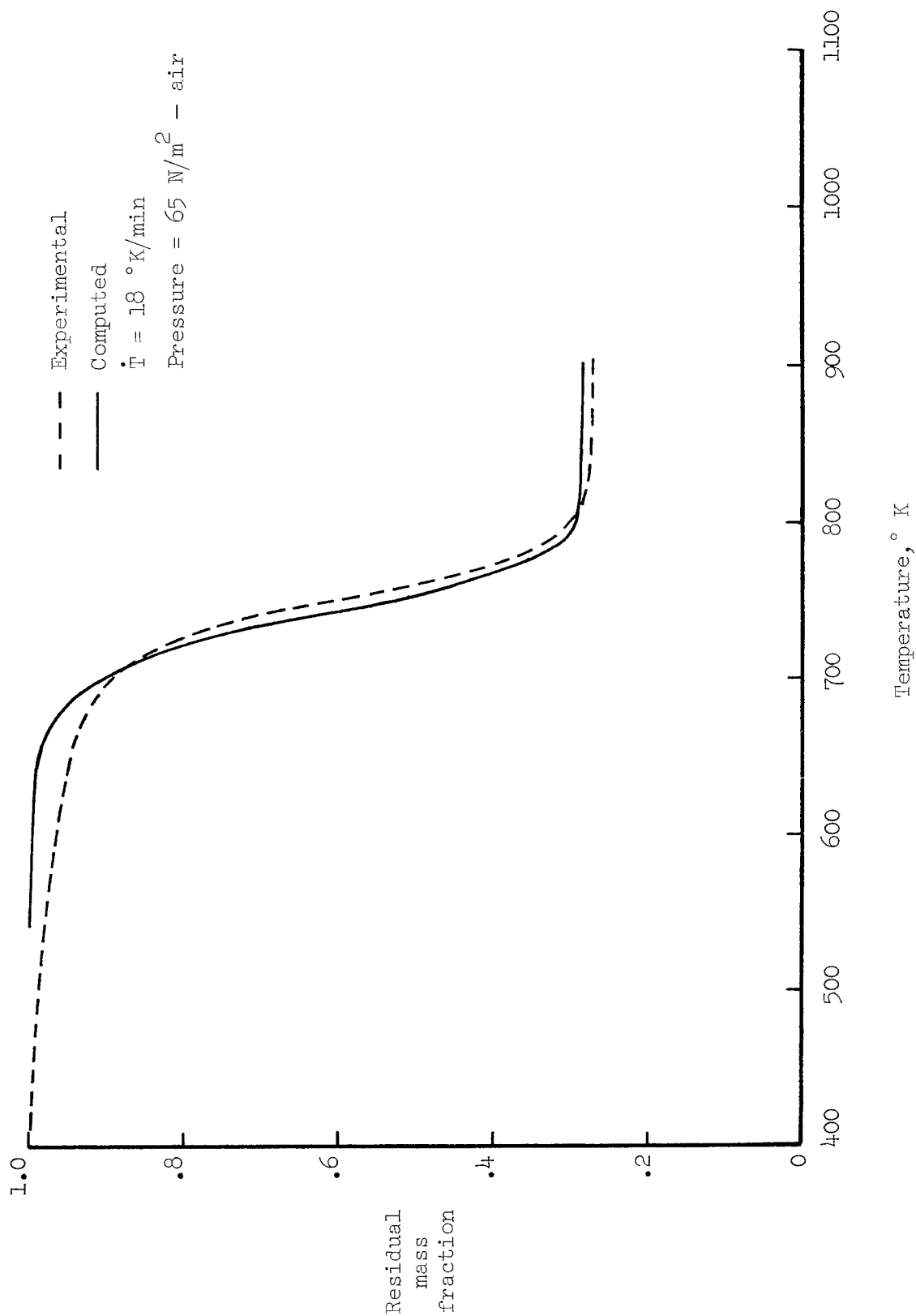


Figure 18.- Experimental and computed TGA plots for a phenolic-silicone composite.



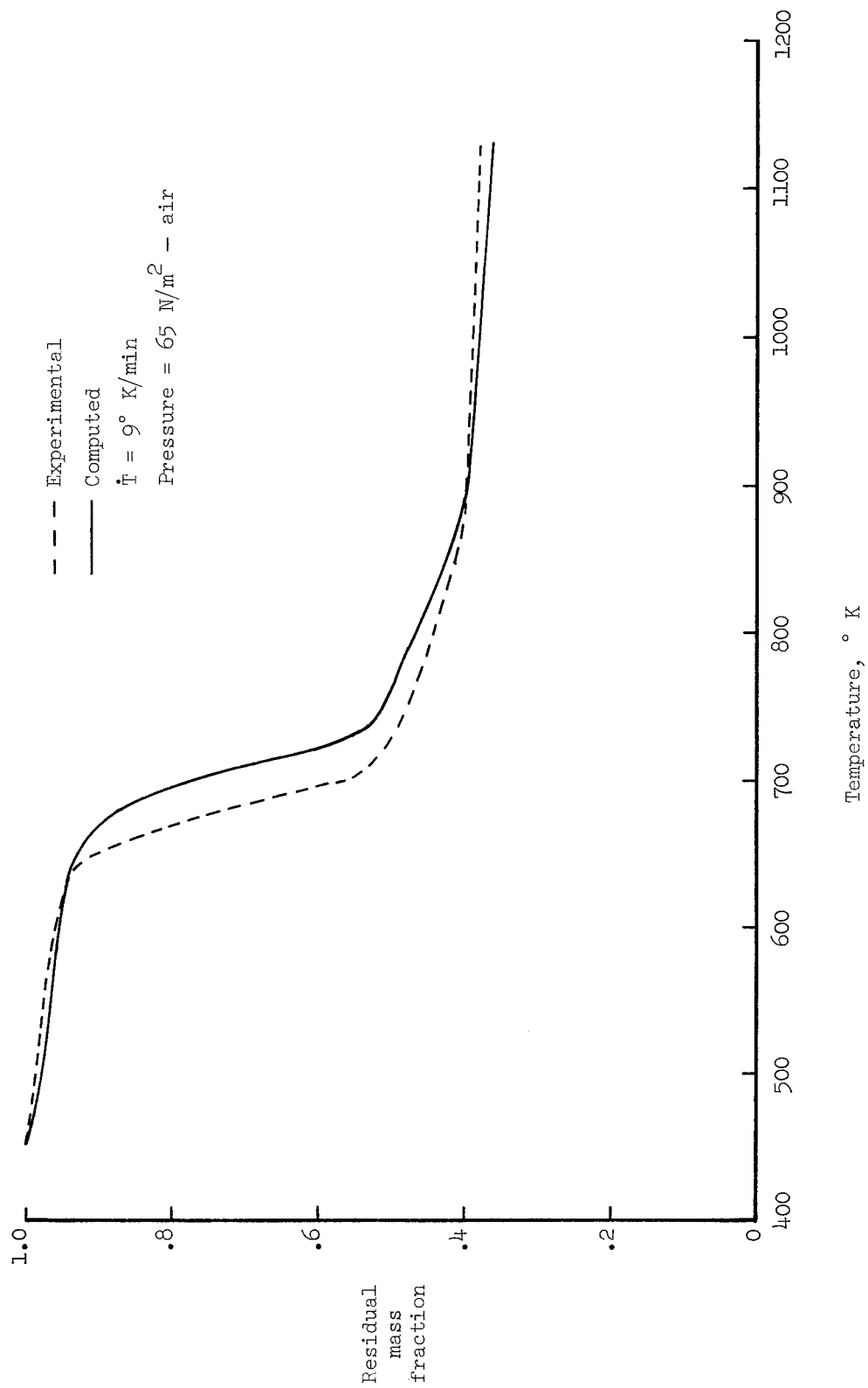


Figure 19.- Experimental and computed TGA plots for a phenolic-nylon composite.

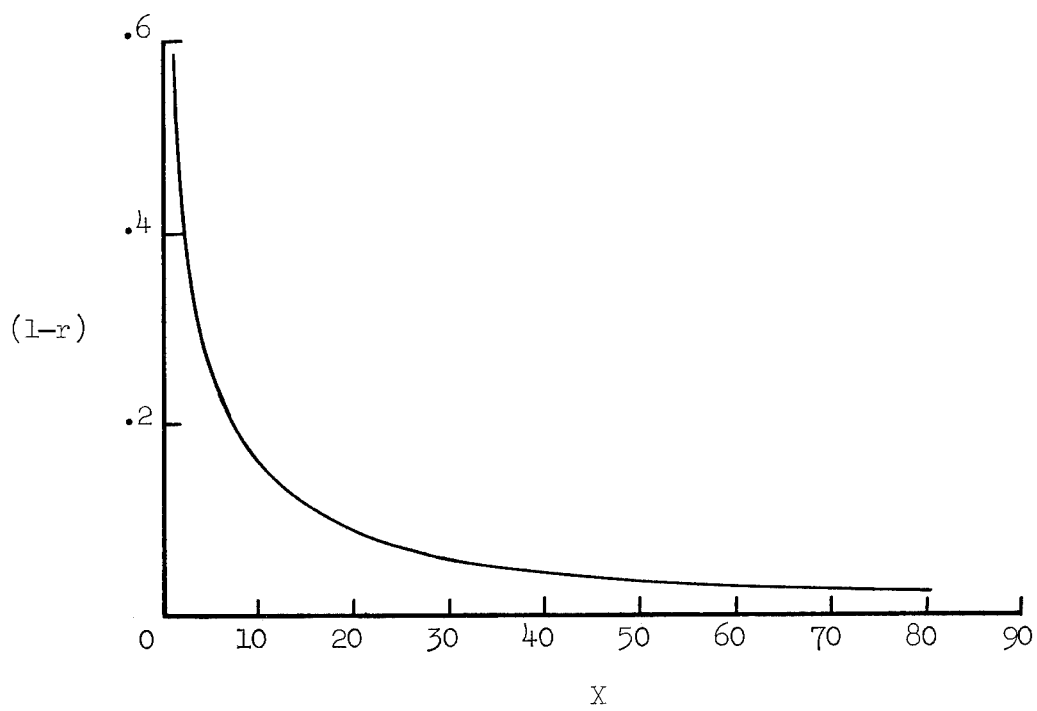


Figure 20.- Relative-error plot involved in using the integral method.

*"The aeronautical and space activities of the United States shall be conducted so as to contribute . . . to the expansion of human knowledge of phenomena in the atmosphere and space. The Administration shall provide for the widest practicable and appropriate dissemination of information concerning its activities and the results thereof."*

—NATIONAL AERONAUTICS AND SPACE ACT OF 1958

## NASA SCIENTIFIC AND TECHNICAL PUBLICATIONS

**TECHNICAL REPORTS:** Scientific and technical information considered important, complete, and a lasting contribution to existing knowledge.

**TECHNICAL NOTES:** Information less broad in scope but nevertheless of importance as a contribution to existing knowledge.

**TECHNICAL MEMORANDUMS:** Information receiving limited distribution because of preliminary data, security classification, or other reasons.

**CONTRACTOR REPORTS:** Scientific and technical information generated under a NASA contract or grant and considered an important contribution to existing knowledge.

**TECHNICAL TRANSLATIONS:** Information published in a foreign language considered to merit NASA distribution in English.

**SPECIAL PUBLICATIONS:** Information derived from or of value to NASA activities. Publications include conference proceedings, monographs, data compilations, handbooks, sourcebooks, and special bibliographies.

**TECHNOLOGY UTILIZATION PUBLICATIONS:** Information on technology used by NASA that may be of particular interest in commercial and other non-aerospace applications. Publications include Tech Briefs, Technology Utilization Reports and Notes, and Technology Surveys.

*Details on the availability of these publications may be obtained from:*

SCIENTIFIC AND TECHNICAL INFORMATION DIVISION  
NATIONAL AERONAUTICS AND SPACE ADMINISTRATION

Washington, D.C. 20546